Final Design and Testing of Blast Mitigating Roller Shutter Door

Phase 2 Summary Report

ABS Consulting Project Number 4456444

March 31, 2022

Prepared for:

Gliderol Doors (S) Pte Ltd

Prepared by:

Matthew J. Kraemer, P.E.
Lead Engineer

Jerry W. Collinsworth
Principal Engineer

Approved by:

Darrell D. Barker, P.E. CP (Blast)
Vice President
Advanced Engineering

Table of Contents

1 Design Development

A blast mitigating roller shutter door design development program was completed by ABS Consulting for Gliderol Doors (S) Pte. Ltd (Gliderol). Gliderol desired to develop a door with two performance levels (PL):

- PL 1 Blast Mitigating Shutter – Door is retained at the top and free at the bottom to minimize reactions on the building structure. Door does not become a source of debris under a blast load
- PL 2 Blast Resistant Shutter – Door is retained at top and bottom and has limited permeant damage. Door can deform substantially but remain attached during the entire duration of the response.

The program consisted of two phases: concept development and detailed design and testing. The concept development was previously completed by ABS Consulting in March 2020. The detailed design and test phase has been completed and is the subject of this report.

2 Door Configuration

The geometry of the roller shutter door was generated based on drawings provided by Gliderol. The overall clear opening dimension of the door was 3.7 m wide and 5.0 m tall. An elevation of the door is shown in Figure 1.

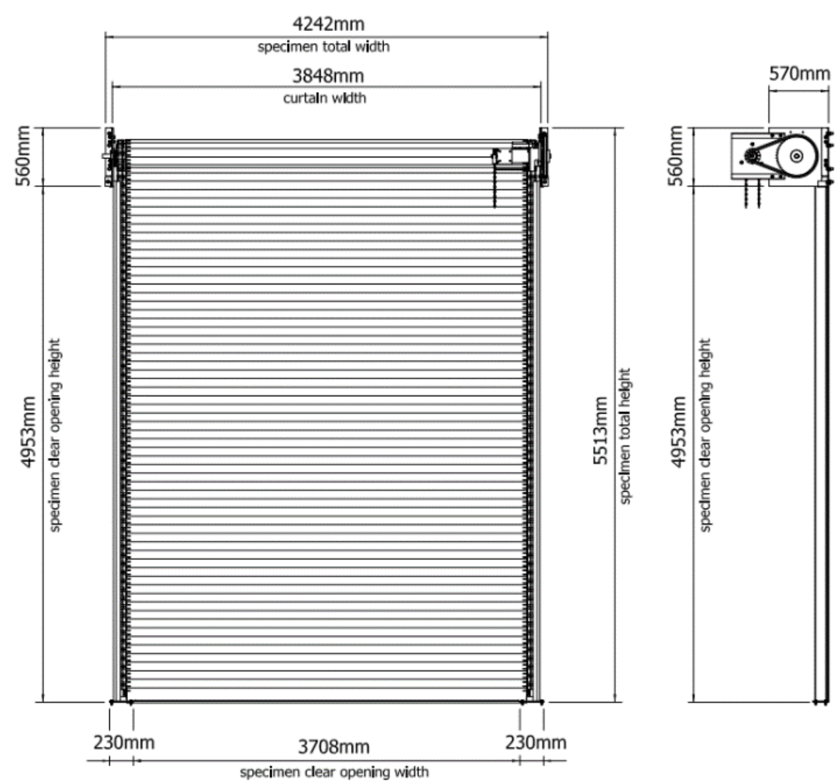

Figure 1. Test Door Dimensions

3 Shock Tube Testing

ABS Consulting conducted Phase 2 blast testing of the Roller Shutter Doors. Two complete door systems were tested in the 12-ft. wide X 16-ft tall test fixture. Testing was conducted at the ABS Consulting facilities at 9092 Green Road, Converse, Texas, USA March 2-4, 2022.

3.1 Test Approach

Blast loads were applied using a "shock tube" as shown in Figure 2. This device uses a sudden burst of compressed air to create a blast pulse, which travels down the tube and is applied to the test specimen which is secured to the end of the tube. The blast load creates a specified positive blast pressure and impulse on the test specimens.

Figure 2. ABS Consulting Shock Tube Apparatus

3.2 Test Articles and Mounting

The tested door systems were all nominally 4953 mm (195-in) tall and 3848 mm (151-in) wide. An isometric view of the roller shutter door system is shown in Figure 3. Doors were attached to a rigid steel reaction frame located at the end of the shock tube. Elevation and plan views of the reaction frame are shown in Figure 4and Figure 5.

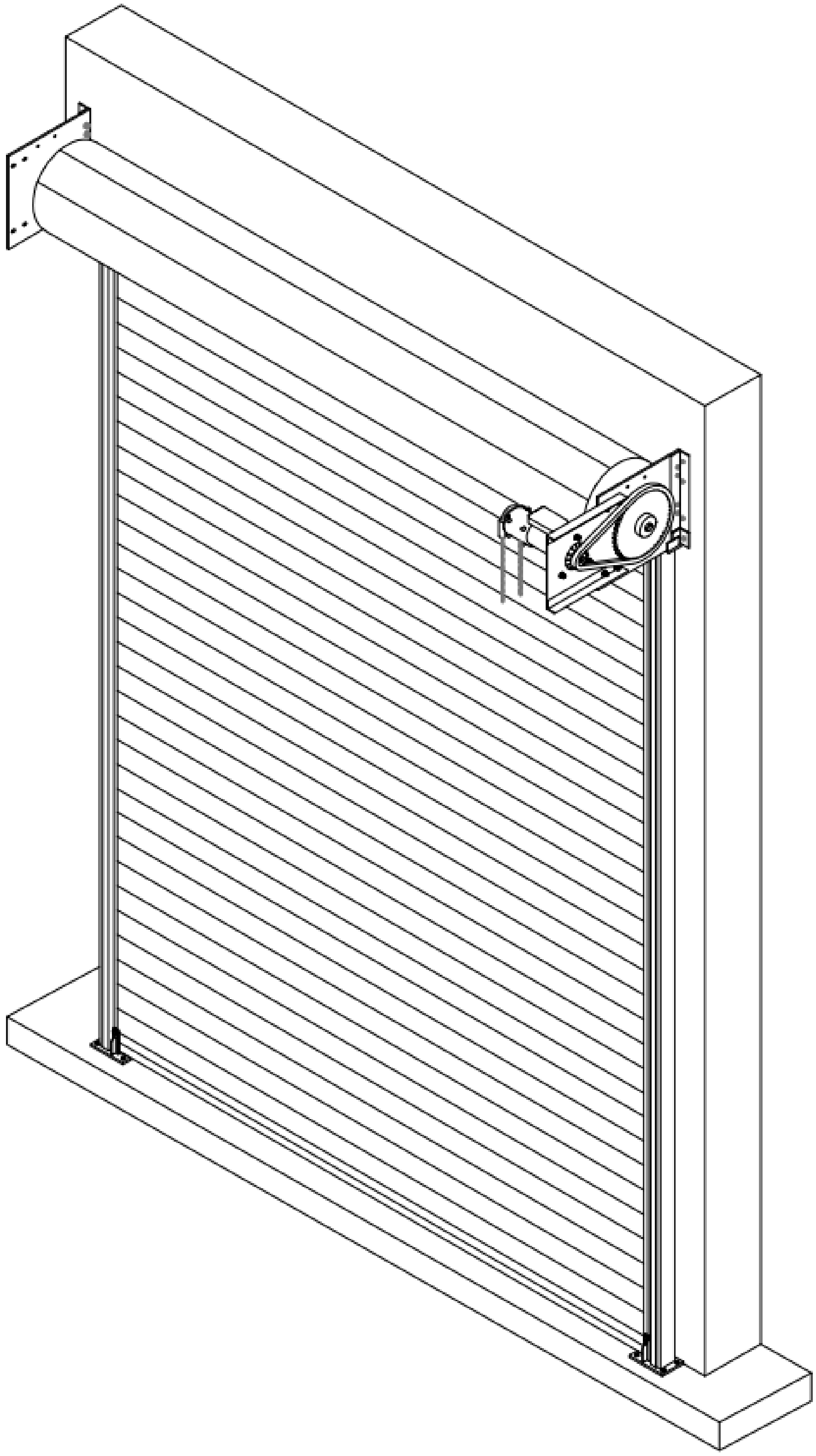

Figure 3. Isometric View of Roller Shutter Door System

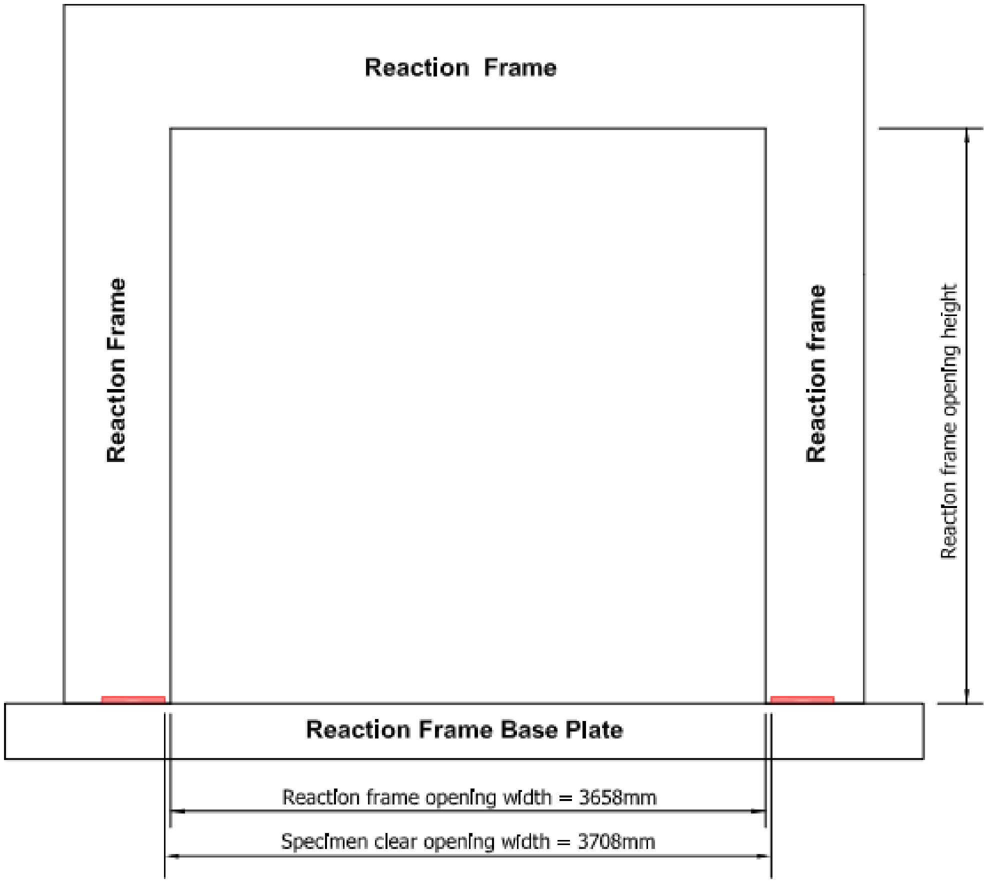

Figure 4. Test Article and Reaction Frame Dimensions – Elevation

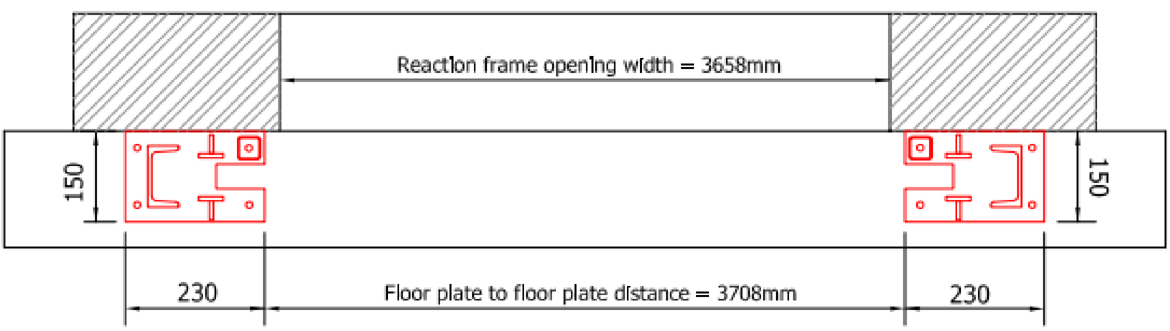

Figure 5. Test Article and Reaction Frame Dimensions – Plan

Roller shutter door assemblies were fixed to the shock tube reaction frame with steel angles attached to the drum mounting brackets (Figure 6). The angles were 10mm thick mild steel. Four M16 bolts connected the angle to each end-plate and four M16 bolts connected the other angle leg to the face of the reaction frame.

Vertical steel door guides were located on each side of the roller shutter curtain that captured the cable termination blocks and show, as shown in Figure 7. Each guide was bound laterally by the drum end-plates and connected to the reaction structure jambs with a single M16 bolt at the top of the guide as show in Figure 8. The bottom of the guides was restrained by slots cut through the thickness of each baseplate that the guide channels nested into. The baseplates were bolted to rigid shelf supports on the face of the shock tube reaction frame with four M12 bolts. Figure 9 shows the baseplate connection and the guide channel bottom connection.

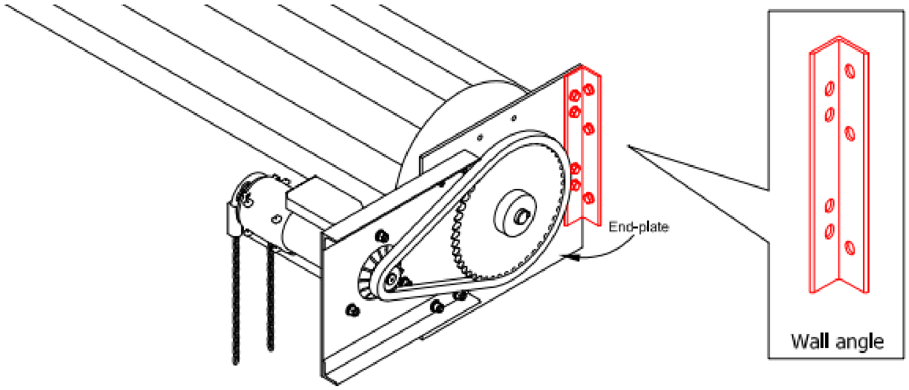

Figure 6. Connection Between Drum End-Plate and Reaction Frame

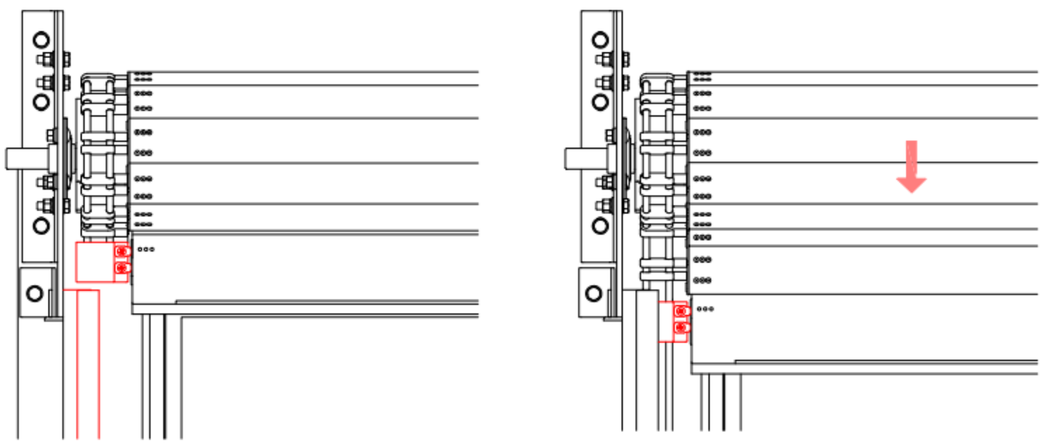

Figure 7. Door Shoe Insertion into Guide

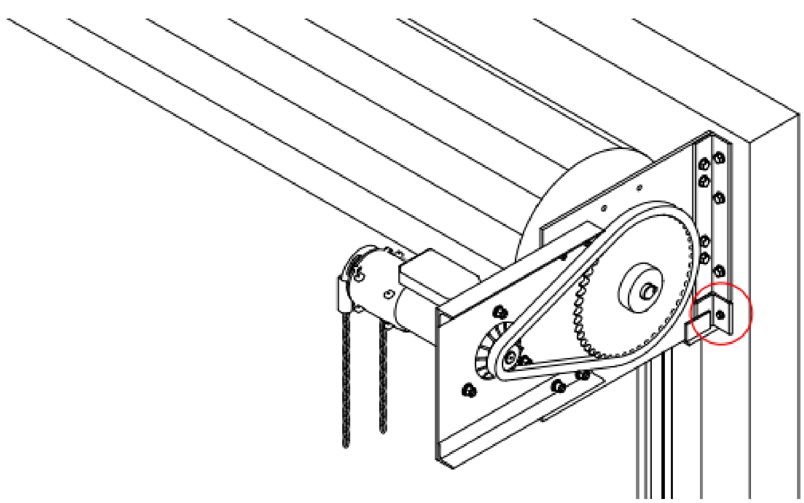

Figure 8. Door Guide Top Connection

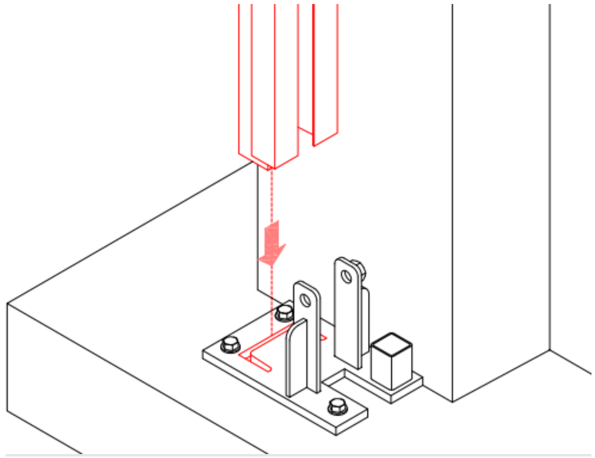

Figure 9. Baseplate and Door Guide Connection

The baseplate included two stiffened tie-down lugs welded to the baseplates to secure the restraining pin. In the PL 1 configuration, the restraining pin was not installed and the panels were free to ride up the door guides, as shown in Figure 10. For the PL 2 configuration, the lift cable shoes were restrained to the base plate by a M16 shear bolt installed through tie down lugs and shown in Figure 11.

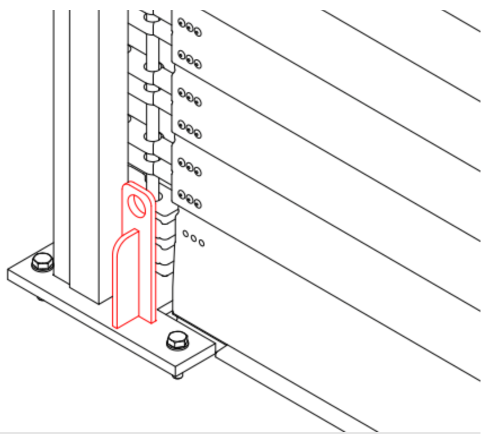

Figure 10. Tie Down Lugs Welded to Baseplate

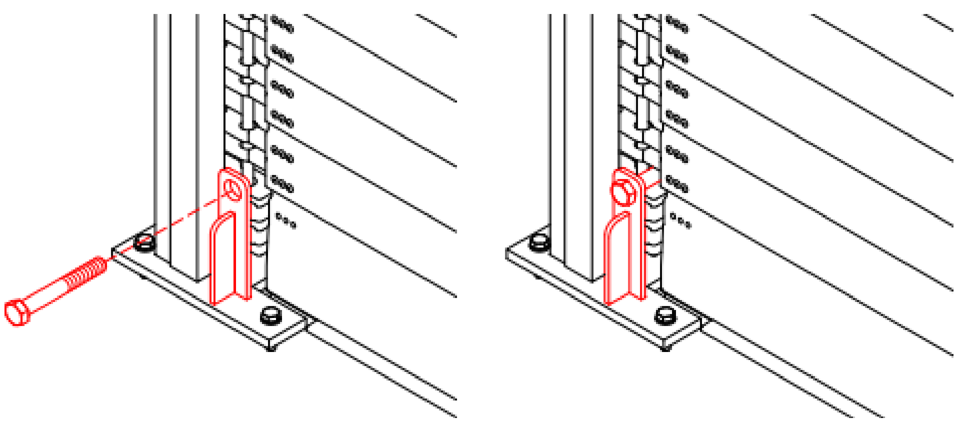

Figure 11. Shear Bolt Installation for PL-2 Condition Only

3.2.1 Test Article PL 1

The roller shutter door system tested in the PL-1 configuration is shown in Figure 12 through Figure 17. The shear bolt to restrain the curtain to the baseplate was not included for PL-1 as shown in Figure 15.

Figure 12. Elevation - PL 1 Configuration

Figure 13. Roller Shutter Fully Open - PL 1 Configuration

Figure 14. Side View - PL 1 Configuration

Figure 15. View of Left and Right Baseplate – PL 1 Configuration

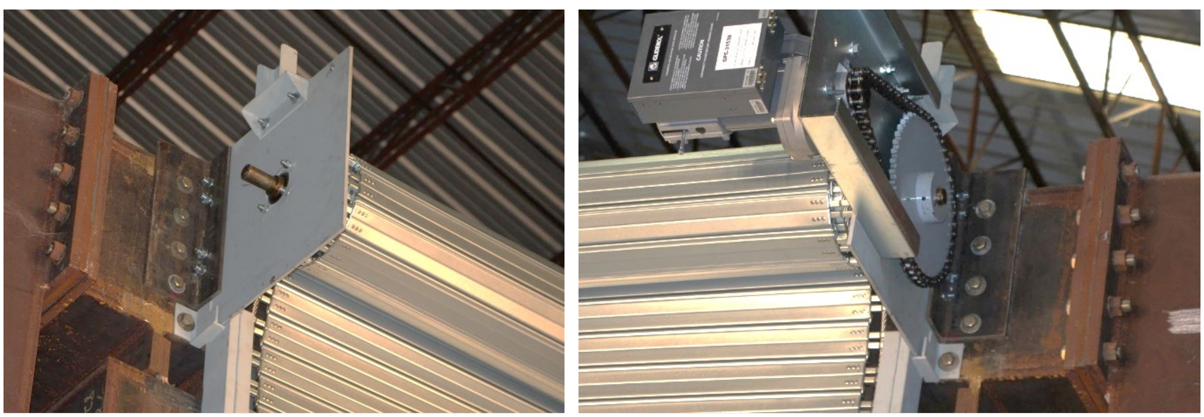

Figure 16. Roller Shutter Mounting

Figure 17. Baseplate Connection

3.2.2 Test Article Configuration PL 2

The roller door system tested in the PL-2 configuration is shown in Figure 18 through Figure 21. The shear bolt to restrain the curtain to the baseplate was included for PL-2 as shown in Figure 21.

Figure 18. Elevation PL 2 Configuration

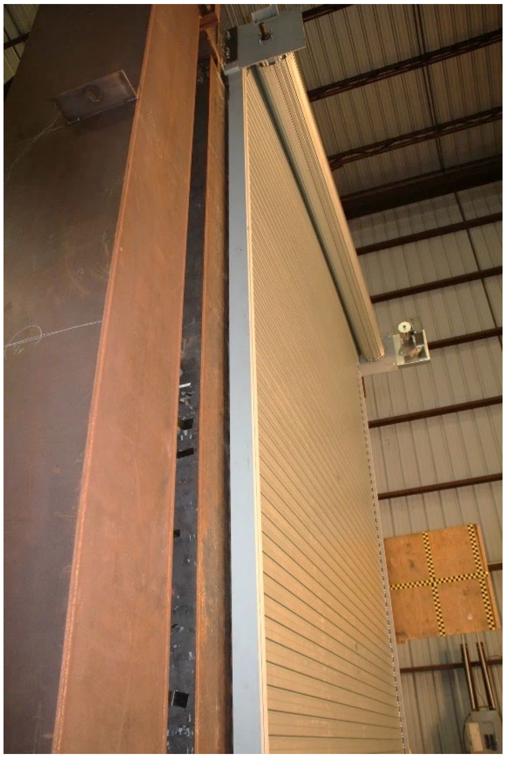

Figure 19. Side View – PL 2 Configuration

Figure 20. View of Curtain Sill – PL 2 Configuration

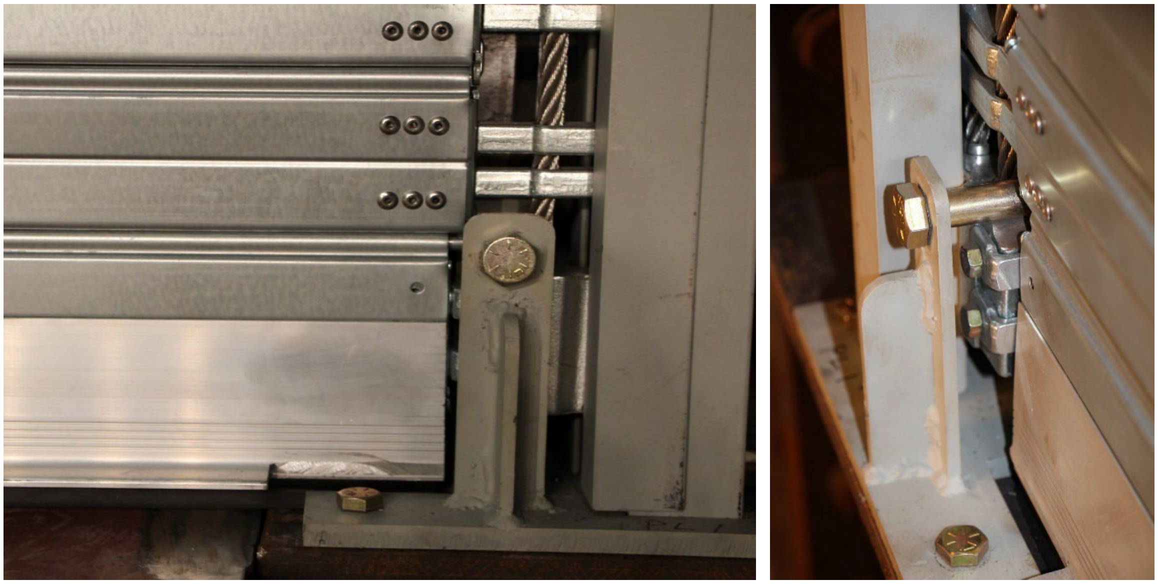

Figure 21. Curtain Shear Bolt Installed – PL 2 Configuration

3.3 Instrumentation

Dynamic pressure gauges were used to measure the applied blast load immediately adjacent to the test specimen. Six gauges (P1-P6) were mounted on the shock tube wall near the loaded plane. A schematic of the shock tube reaction structure and test article that identifies the locations of the pressure gauges is shown in Figure 22. For the calibration shots, five additional gauges were mounted in blanking panels in approximately the same location as the test article. Figure 23 shows an elevation of the blanking panels and the gauge locations.

Dynamic blast pressures gauges were piezoelectric type with a range of 0-100 psi peak pressure. A close-up view of a blast gauge is shown in Figure 24. Pressure waveforms were recorded by a digital oscilloscope sampling at a minimum of 1,000 kHz.

Two high-speed cameras, recording at 1000 frames per second, were used to capture the response of the panel during each test. One camera was positioned at an oblique angle to view the overall response of the test articles. The second was positioned parallel to the door panel face to capture the mid-span deflection of the panel during each test. The view included fiduciary markings to provide a scale in the video. Reference scales placed at the panel centerline were included in separate calibration videos taken prior to the shock tube tests.

PCC software was used to calculate the peak deflection of the panels from the high-speed video. A measurement scale was defined by the calibration videos and fiduciary grid. The position of the panels point of maximum deflection in each frame was measured in the PCC software to calculate the ultimate peak deflection during each test.

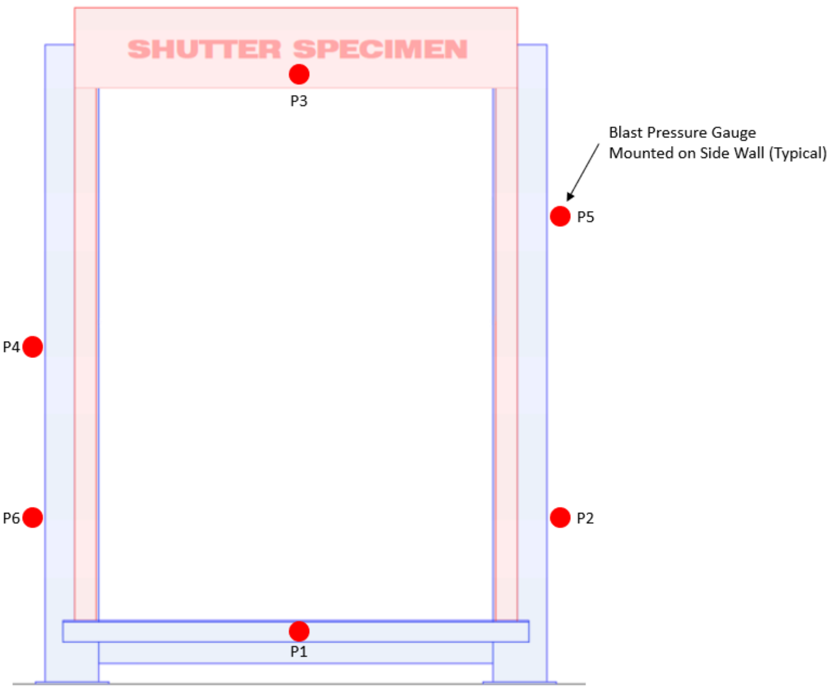

Figure 22. Testing Gauge Locations

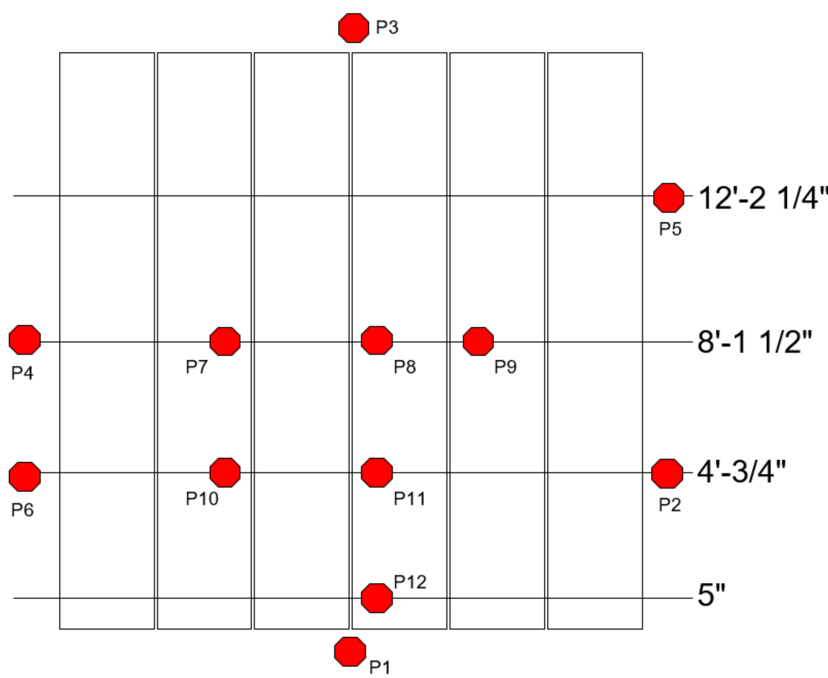

Figure 23. Blanking Panel Gauge Locations

Figure 24. Blast Pressure Gauge

3.4 Blast Load

A pressure-time history for gauges in the calibration test (Test 085) and Test 01 of the Roller Shutter Door system (PL 2 configuration) is shown in Figure 25. Calibration test (Test 086) and Test 04 of the Roller Shutter Door system (PL 1 configuration) is shown in Figure 26.

The impulse is computed by integrating the pressure-time history. The pressure trace for the calibration test dips to zero and exhibits some secondary pressure spikes. The initial and secondary pressure excursions are included in the impulse computation, since the test article has a maximum response time longer than the duration of the load, and thus all of the pressure-time history will contribute to the ultimate deflection.

As seen in the figures below, the impulse values recorded for test shots are considerably lower than the impulse values from the calibration shot, even though the same blast pulse was generated by the shock tube driver. The difference in impulse is due to the displacement of the test article, which allows the blast load measured by the gauges to vent. This reduction is inherent in the energy absorbing test article response, thus the measured impulse on the test article will always be less than the measured impulse on a rigid wall. The blast load “clears” the gauge quickly due to the deflection of the roller panel slats and does not capture the full energy imparted to the test article. For this reason, the applied load from the calibration test, rather than the recorded load from the specimen tests, is used for the rated blast load.

For the PL 2 configuration in Test 01, the calibration test had an average peak pressure of 4.5 psi (31.2 kPa) and an average applied impulse of 47 psi-ms (326 kPa-ms). For PL 1 configuration in Test 03, the calibration test had an average peak pressure of 10.2 psi (70.3 kPa) and an average applied impulse of 159 psi-ms (1096 kPa-ms).

The blast loads shown for each test described in the following sections are from the calibration tests as these show the load applied to the door without consideration of the venting created by the door response.

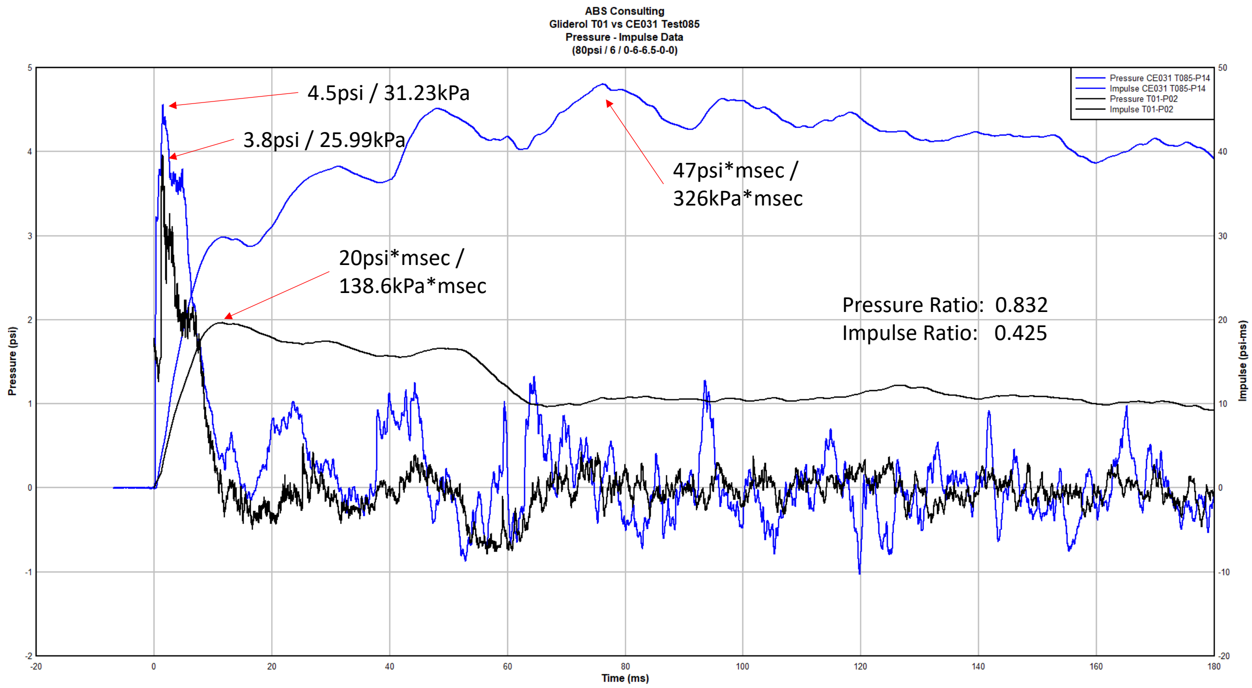

Figure 25. Pressure-Time History – Calibration and Test 01

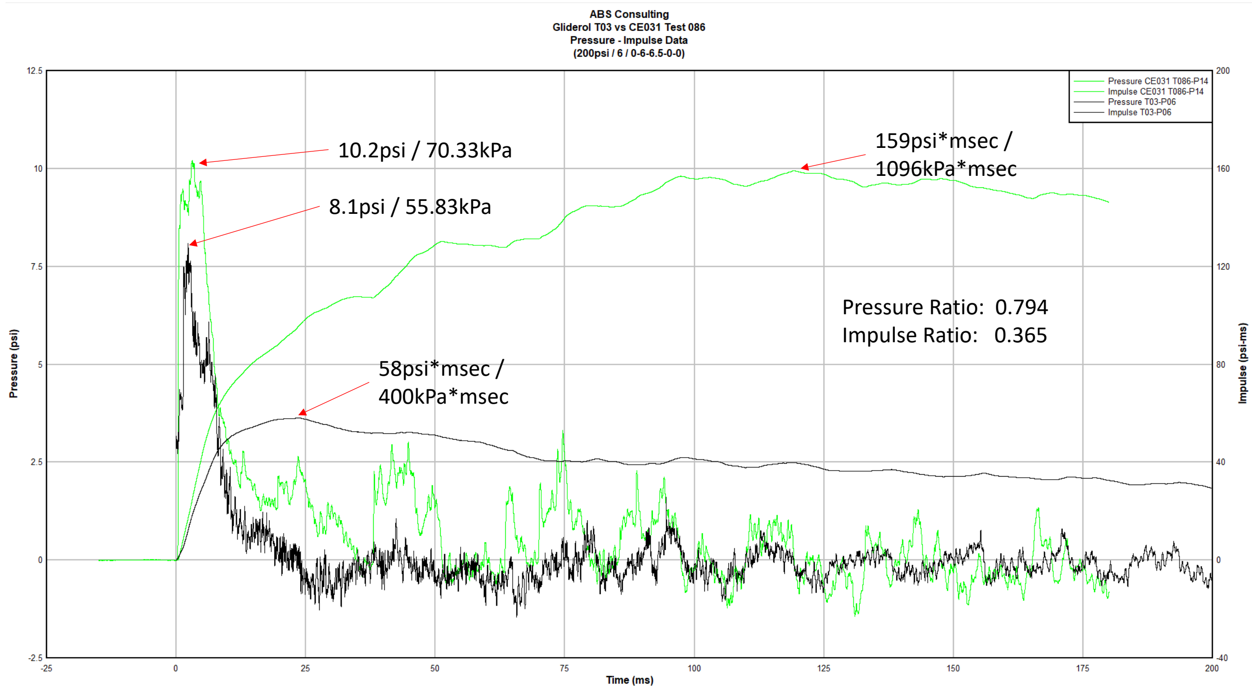

Figure 26. Pressure-Time History - Calibration and Test 03

3.5 Test Results

A total of 5 tests were conducted on 2 test articles. Photographs were taken of test specimens and the test setup prior to and following each test to document the performance.

3.5.1 Test 01

Test 01 was the first test conducted and was configured as a PL 2. The applied load on the door from Calibration Test 085 is 31.2 kPa (4.5 psi) and an average applied impulse of 326 kPa-ms (47 psi-ms) as shown in Figure 27. The door curtain deflected uniformly until arrested by the restraining lug. A maximum deflection of 489 mm (19.3 in) was reached at 136 ms. The door curtain sustained minor permanent damage and was operable after the test. No damage to the restraint lugs or bolts was noted. No breakage of the cables or outer strands was observed. Minor damage to some of the 8 mm rods through the door panels was noted. There was no damage to the drum or supports. The door curtain extended approximately 40 mm downward due to rotation of the drum. No failures of the door system or support framing were noted post-test. An overall view of the post-test condition of the article is shown in Figure 28. A close-up of the condition of both sides of the panels is shown in Figure 29. Figure 30 shows the condition of the baseplates, shear bolts and curtain shoes. Views of the door panel deflection taken from the high-speed video are shown in Figure 31 and Figure 32.

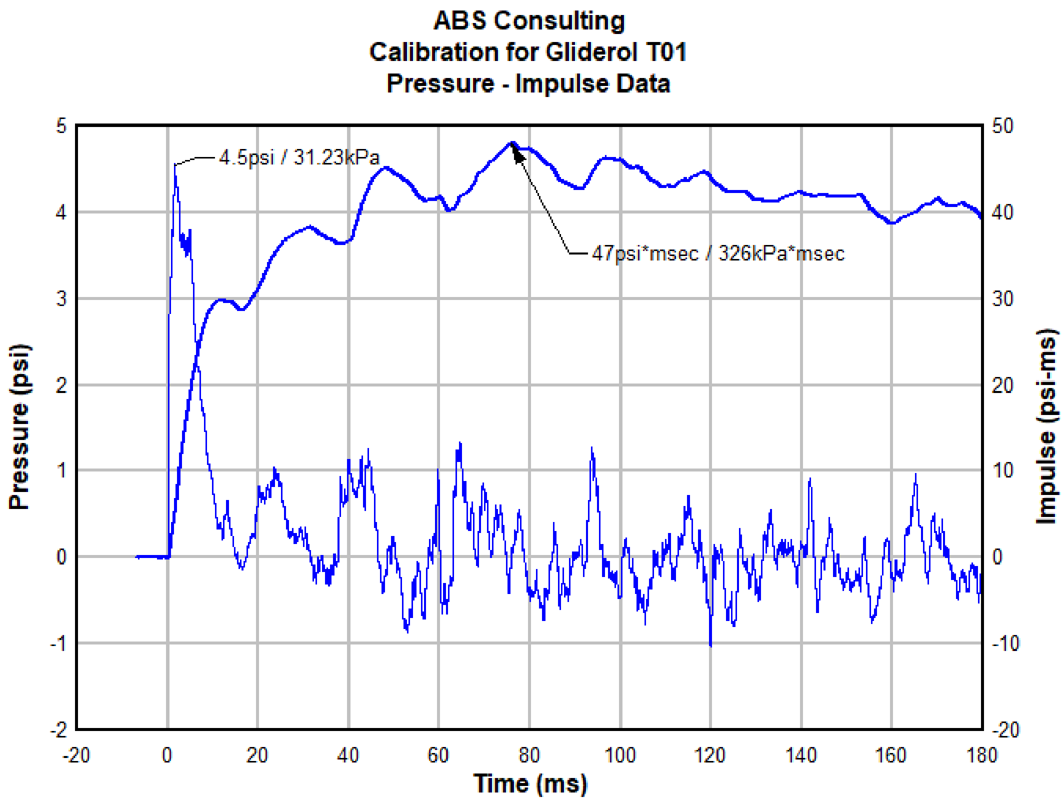

Figure 27. Applied Blast Load Test 01

Figure 28. Test 01 - Post-Test Photo of Test Article

Figure 29. Test 01 - Post-Test Photos of Shutter Sides

Figure 30. Test 01 - Post-Test Photos of Curtain Shoes

Figure 31. Test 01 - Point of Maximum Deflection (Oblique View)

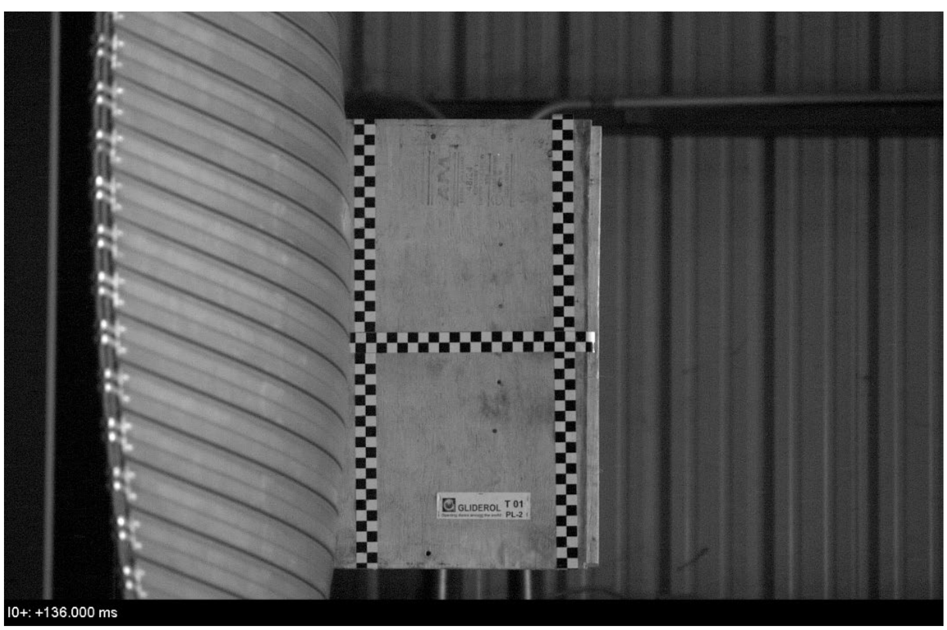

Figure 32. Test 01 - Point of Maximum Deflection (Side View)

3.5.2 Test 02

Test 02 was the second test conducted on the first test article, a PL 2 Configuration. Before the test, the cables and slat rod termination connectors were reinserted into the guide rails, and the drum was rotated to take up slack in the curtain which occurred during the prior test. The applied load was an average pressure of 39.3 kPa (5.7 psi) and an average impulse of 502.6 kPa-ms (72.9 psi-m) based on the calibration test. The pressure-time history is shown in Figure 33. The door curtain deflected uniformly until restrained by the cables and restraining lugs. A maximum deflection of 791 mm (31.2 in) was recorded at 116 ms. The panel was moderately deformed but remained intact. Panel slat and internal rod damage was noted in the lowermost portion of the shutter near the baseplates. The cables were deformed at the shoe due to bearing on the shear bolts, but no failures were noted. There was no damage to the drum or supports. The door curtain extended approximately 101 mm downward due to rotation of the drum. No failures of the door system or support framing were noted post-test.

An overall view of the post-test condition of this test article is shown in Figure 34. A close-up of the condition of both sides of the panels is shown in Figure 35. Figure 36 shows the curtain shoe and restraining system. A side view of the door panel deflection taken from the high-speed video is shown in Figure 37.

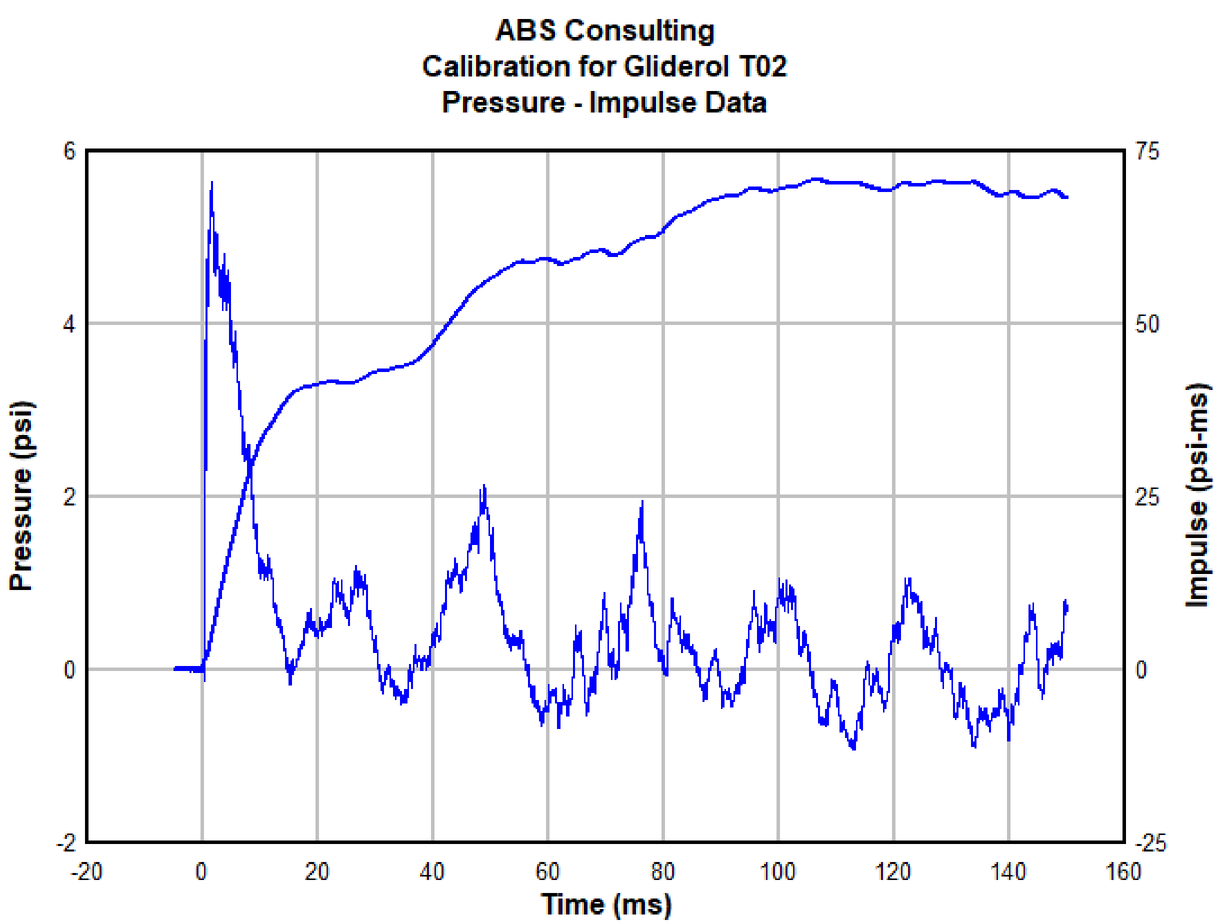

Figure 33. Applied Blast Load Test 02

Figure 34. Test 02 - Post-Test Photo of Test Article

Figure 35. Test 02 - Post-Test Photos of Shutter Sides

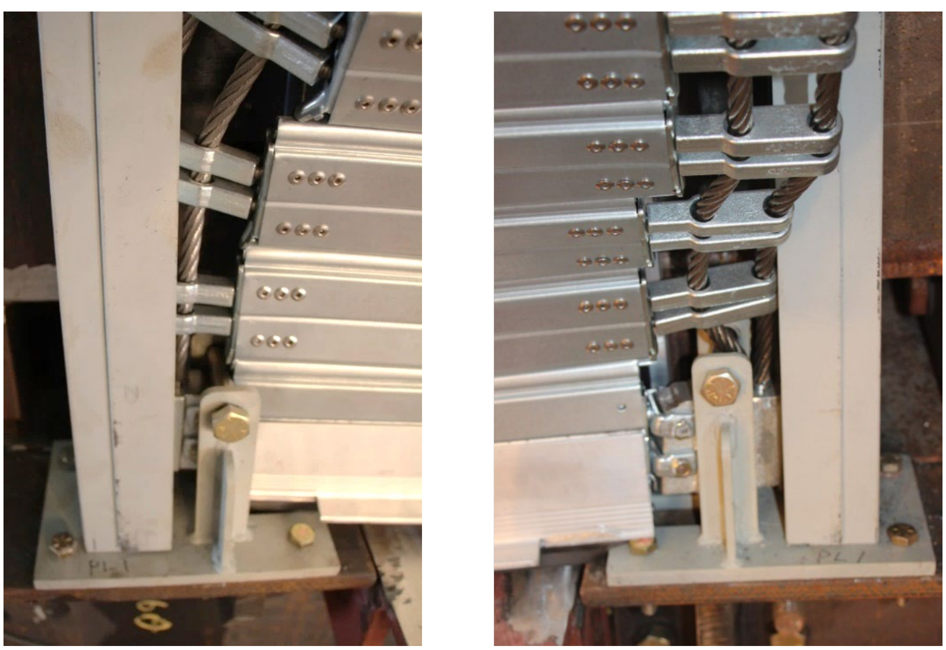

Figure 36. Test 02 - Post-Test Photos of Curtain Shoes

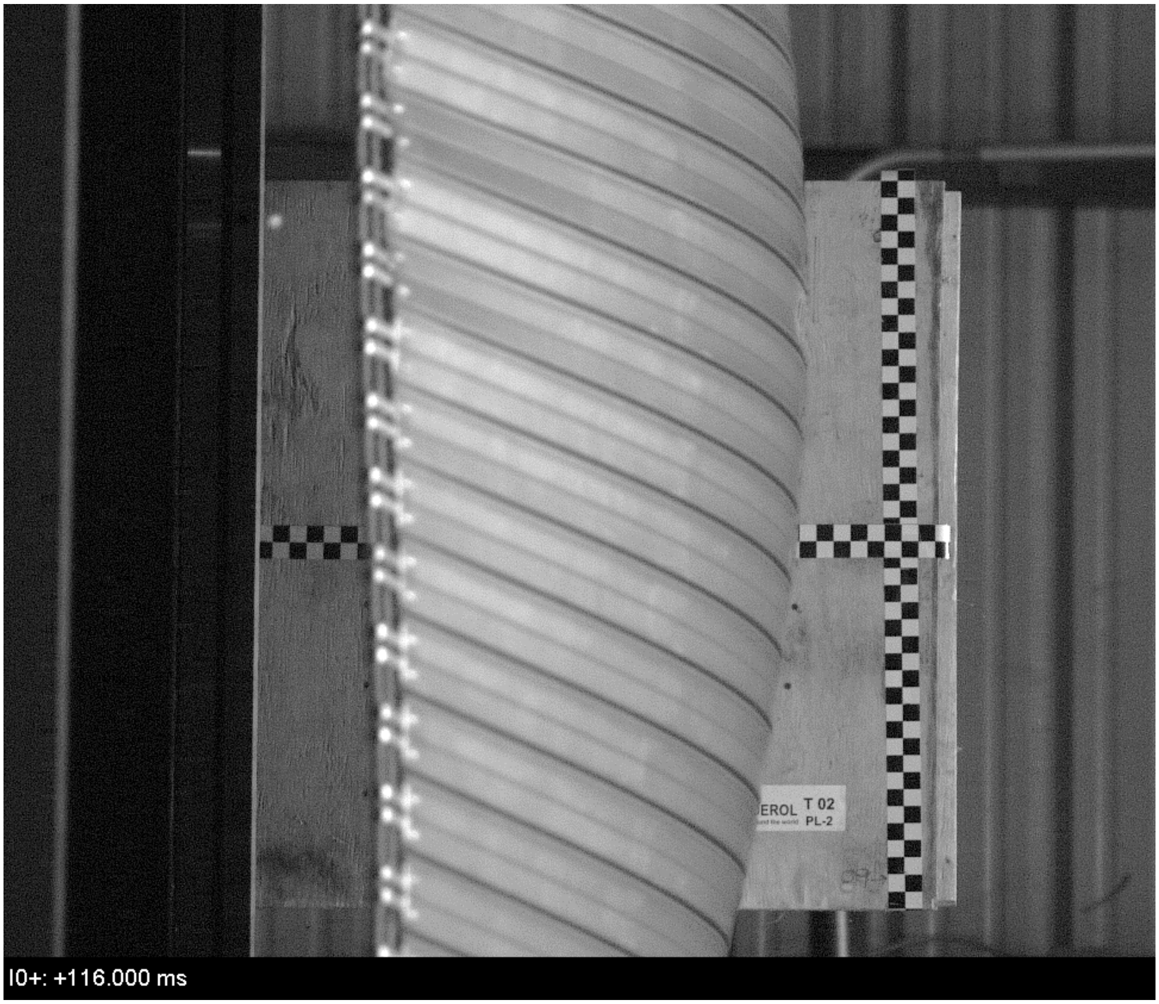

Figure 37. Test 02 - Point of Maximum Deflection (Side View)

3.5.3 Test 03

Test 03 was the third test to be conducted on the first test article, this time in a PL 1 Configuration. The applied load was an average pressure of 65.5 kPa (9.5 psi) and an average impulse of 900.5 kPa-ms (130.6 psi-ms) based on the calibration test. The door curtain shoe released from the guide rails at 32 ms then rotated around the drum with a peak height just above the drum before returning to its original position. There was permanent damage to the door curtain but no failure of the cables or interior support rods for the panels was observed. The door curtain deflected downward 38 mm as the drum rotated. Approximately two full turns of the door curtain remained on the drum.

An overall view of the post-test condition of the article is shown in Figure 39. A close-up of the condition of both sides of the panels is shown in Figure 40. The curtain bottom is shown in Figure 41. An image at 300 ms, taken from the high-speed camera footage of the curtain rotating upwards, is shown in Figure 42.

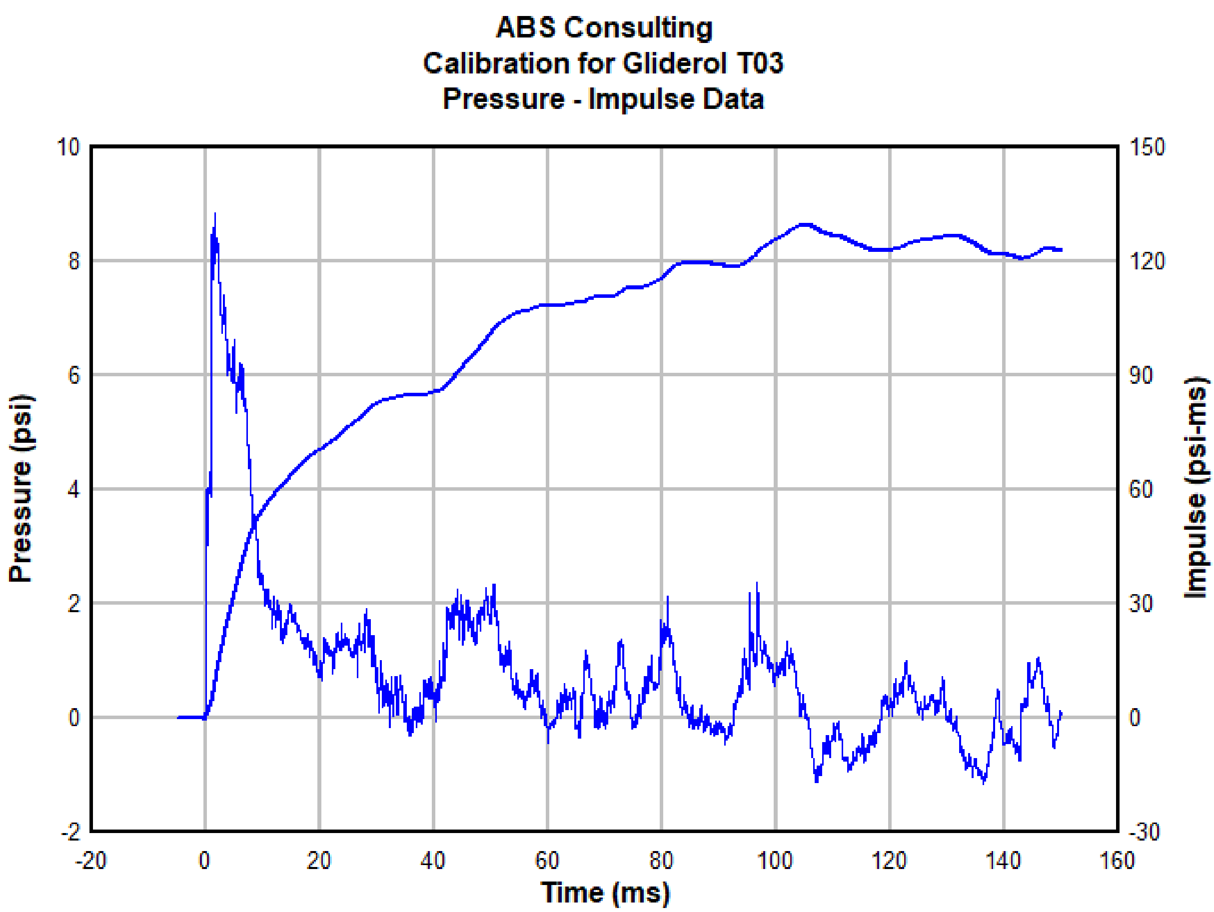

Figure 38. Applied Blast Load Test 03

Figure 39. Test 03 - Post-Test Photo of Test Article

Figure 40. Test 03 - Post-Test Photos of Shutter Sides

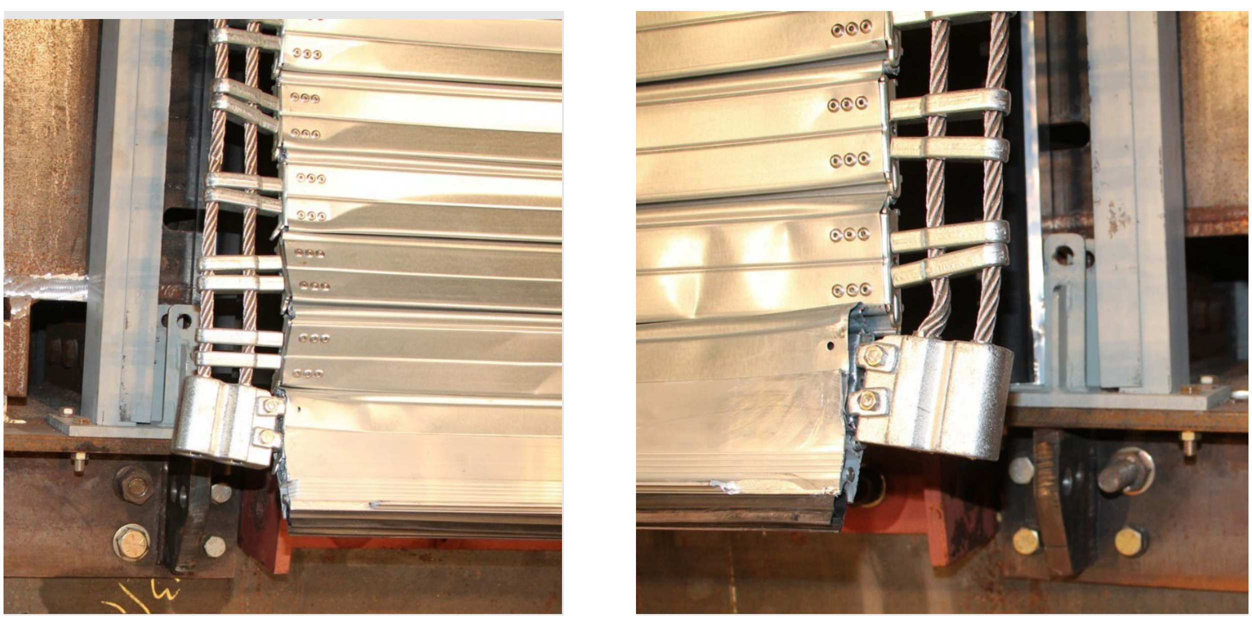

Figure 41. Test 03 - Post-Test Photos of Curtain Bottom

Figure 42: Test 03 - Image from High-Speed Video

3.5.4 Test 04

Test 04 was conducted on a new test article in the PL 1 configuration. The applied load was an average pressure of 75.2 kPa (10.9 psi) and an average impulse of 1046.6 kPa-ms(151.8 psi-ms) based on the calibration test (Figure 43). The door curtain rotated around the drum with a peak height just above the drum before returning to its original position. There was permanent damage to the door curtain but no failure of the cables or interior support rods for the panels was observed. The door curtain deflected downward 202 mm as the drum rotated. Approximately two full turns of the door curtain remained on the drum. An overall view of the post condition of the article is shown in Figure 44. A close-up of the condition of both sides of the panels is shown in Figure 45. The curtain bottom is shown in Figure 46. An image taken from the high-speed video 300 ms into the shutter response is shown in Figure 47.

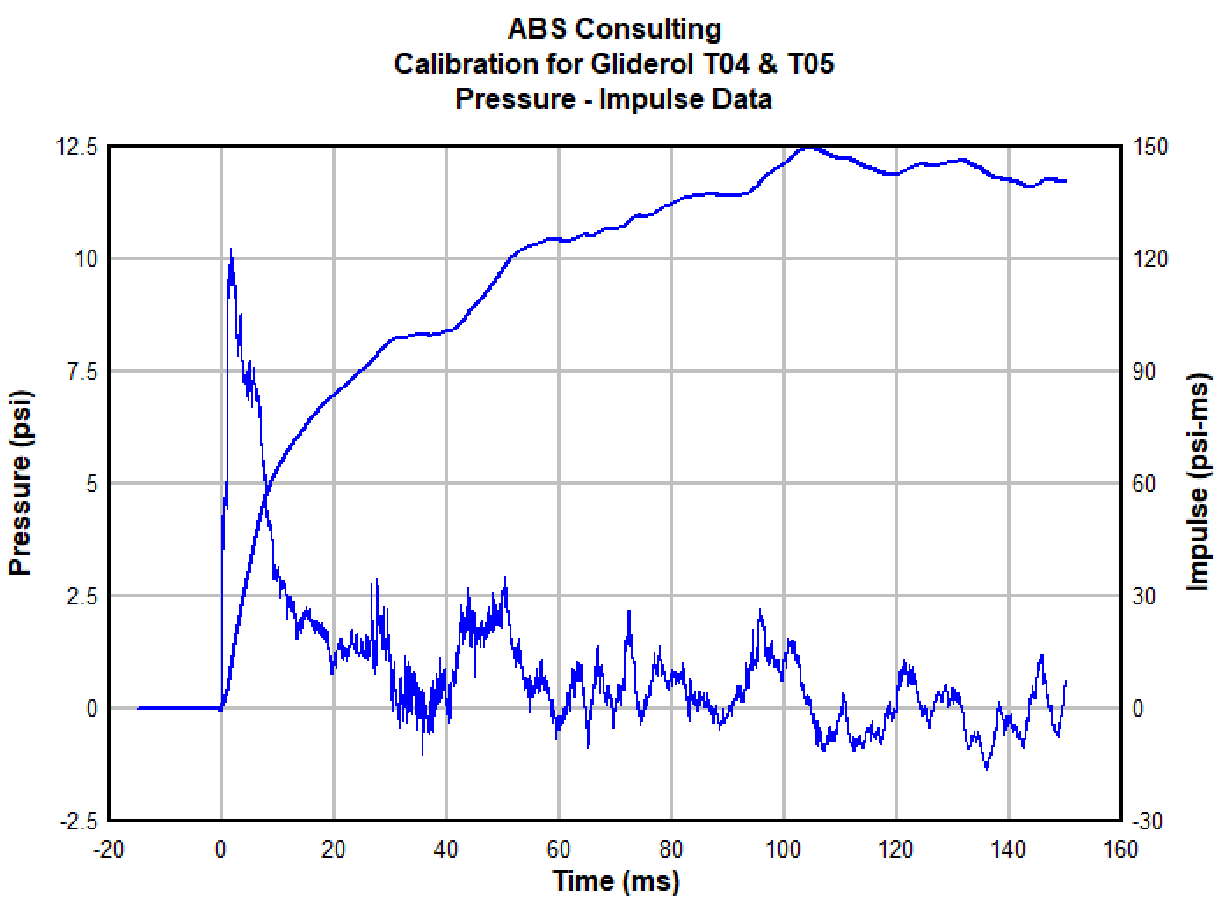

Figure 43. Applied Blast Load Test 04

Figure 44. Test 04 - Post-Test Photo of Test Article

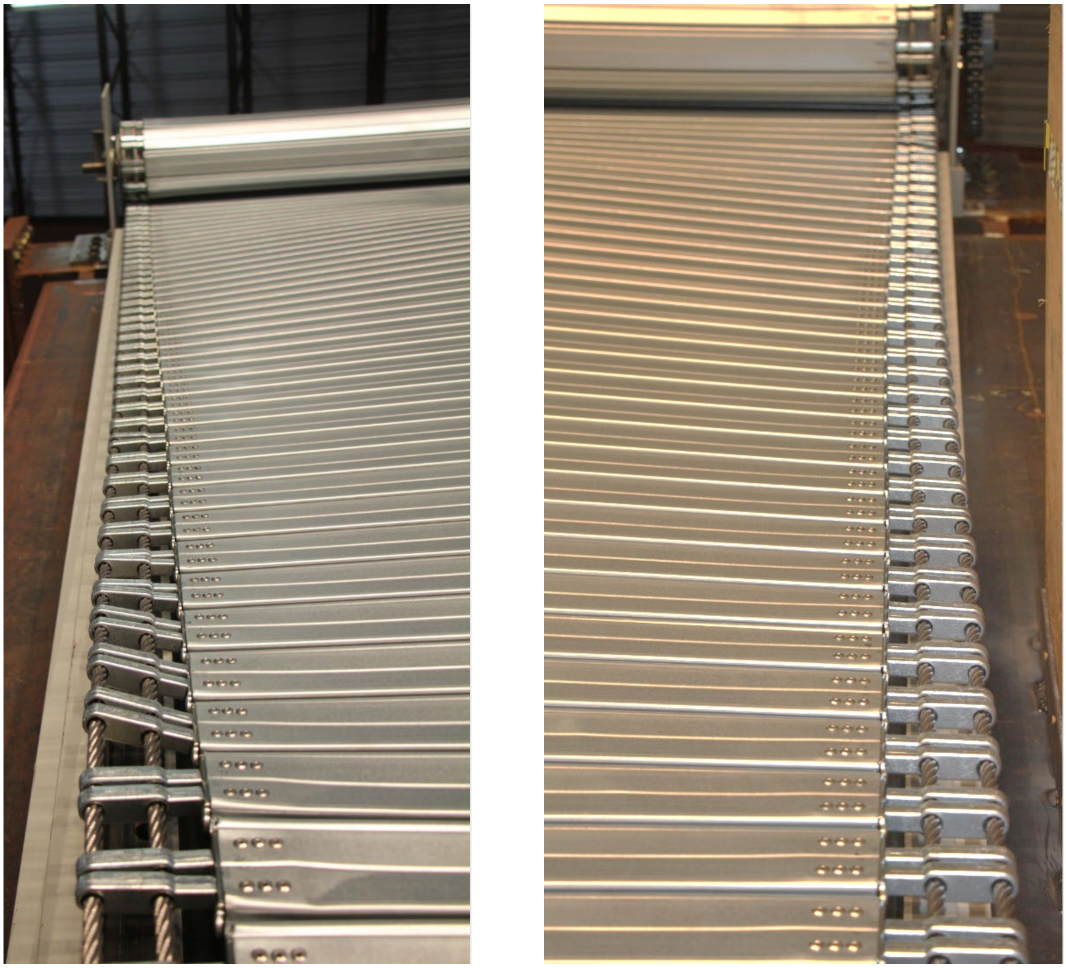

Figure 45. Test 04 - Post-Test Photos of Shutter Sides

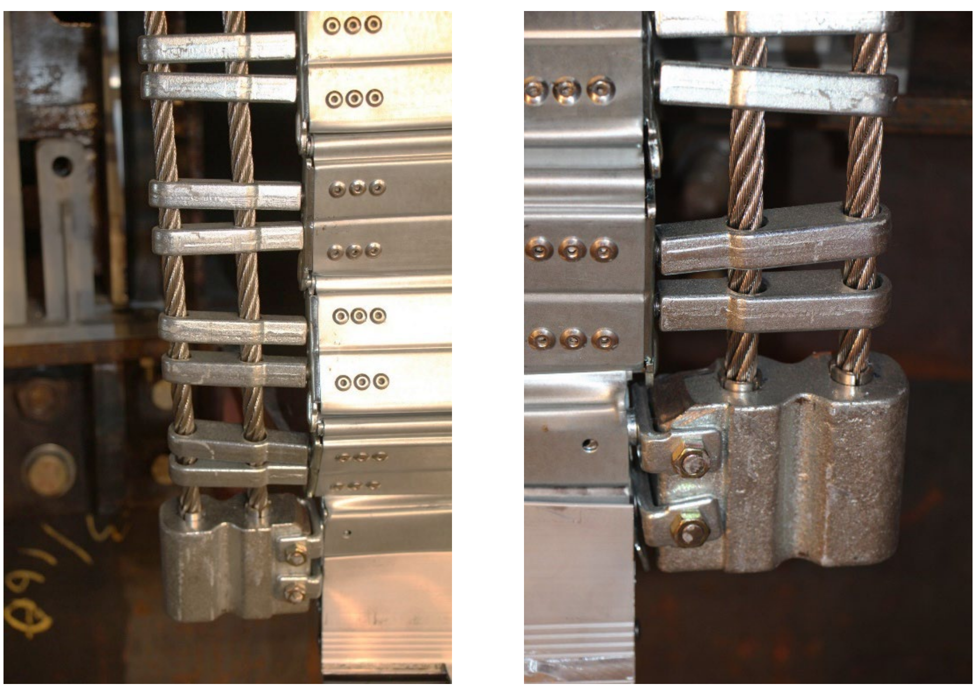

Figure 46. Test 04 - Post-Test Photos of Curtain Bottom

Figure 47. Test 04 - Image from High-Speed Video

3.5.5 Test 05

Test 05 was the second test conducted on the second test article. A PL 2 configuration was used. The applied load was an average pressure of 10.9 psi (75.2 kPa) and an average impulse of 151.8 psi-ms (1046.6 kPa-ms) based on the calibration test shown in Figure 48. This impulse was 350% of the design load for the PL 2 configuration. The door curtain deflected uniformly until restrained by the cables and restraining lugs. A deflection of 461 mm (18.1 in) was recorded at 100 ms at which point the restraining lug on the left side failed at the weld connection to the base plate on the left side. The restraining lug on the right side did not fail. The door curtain continued to deform with a maximum deflection of approximately 2000 mm. The panel was moderately deformed. The drum rotated until all the remaining door curtain unrolled. No damage to the cables or door panels was observed at the drum. The drum axle sheared at the end plate at approximately 48 ms, allowing the drum to unwind. The drum was still supported by the plate and bearing. No debris from the door or hardware was projected.

An overall view of the post-test condition of the test article is shown in Figure 49. Close-up views of the baseplates and curtain shoes are shown in Figure 50 through Figure 53. Images taken from the high-speed video just prior to the failure of the retaining lug (100 ms) is shown in Figure 54. A high-speed image of the curtain response at 350 ms is shown in Figure 55.

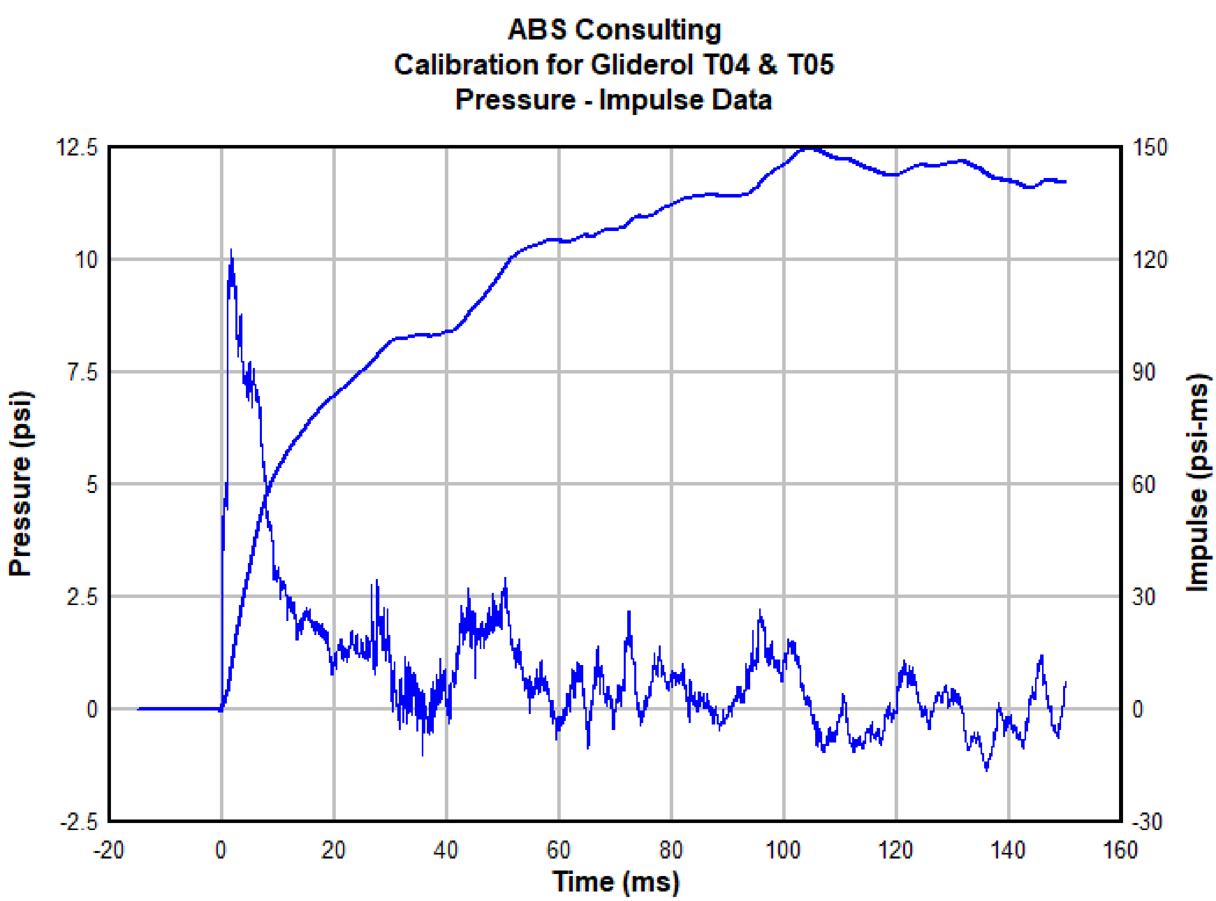

Figure 48. Applied Bast Load Test 05

Figure 49. Test 05 - Post-Test Photo of Test Article

Figure 50. Test 05 - Post-Test Photos of Left Baseplate

Figure 51. Test 05 - Post-Test Photos of Left Curtain Side

Figure 52. Test 05 - Post-Test Photos of Right Baseplate

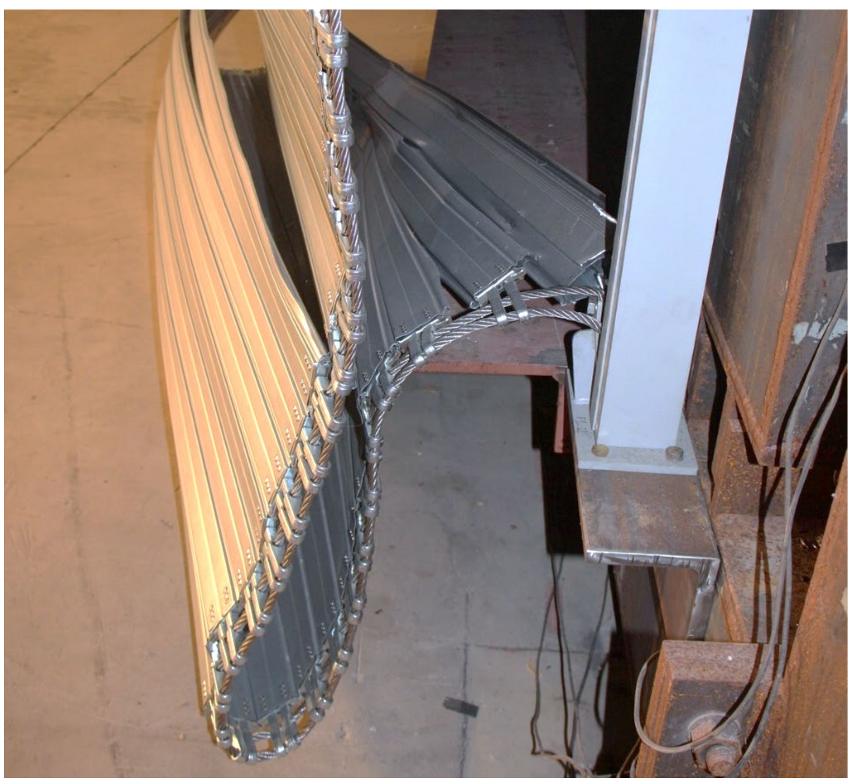

Figure 53. Test 05 - Post-Test Photos of Curtain Shoes

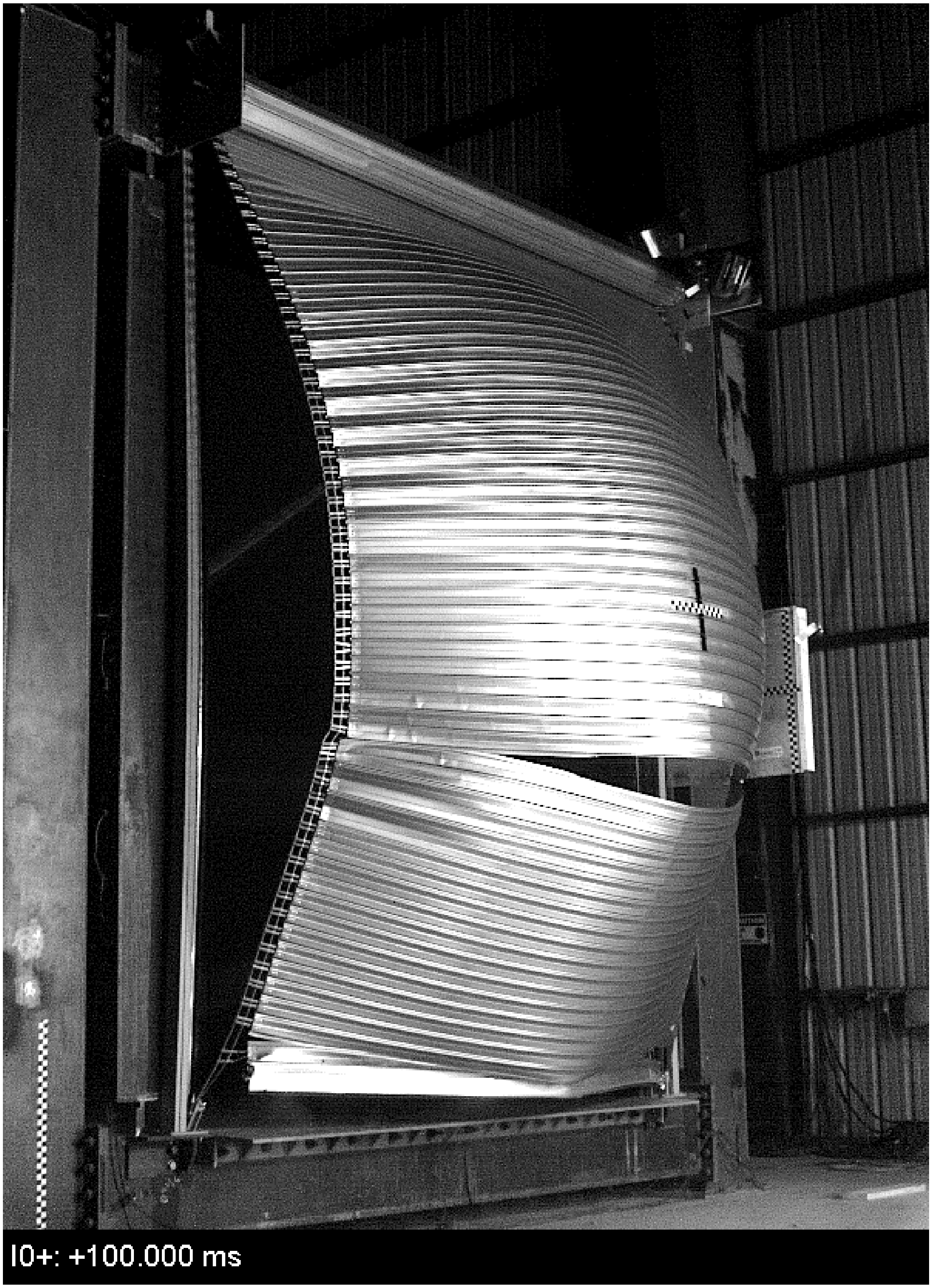

Figure 54. Test 05 - High-Speed Image Prior to Restraint Failure

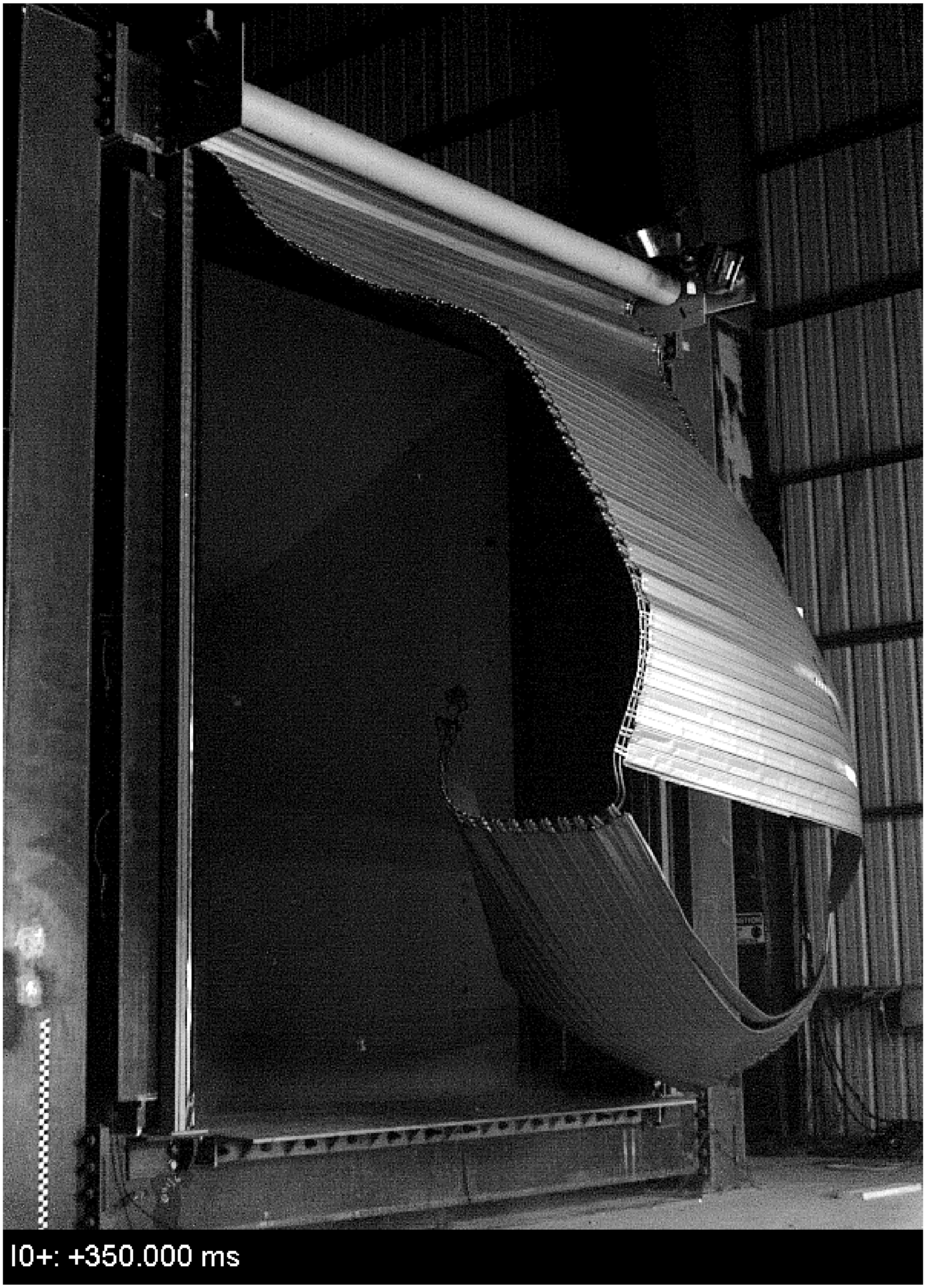

Figure 55. Test 05 - High-Speed Image at 350ms

4 FEA for Test Loads

4.1 PL 1 Simulation for Test 04 Measured Load

A FEA simulation of the PL 1 configuration was prepared for the loads measured by the blast gauges in Test 04. The FEA model of the roller shutter door was developed using an explicit-based, large deformation, dynamic FEA code LS-DYNA R13 (Linux-Version) together with its pre and post-processor LS-PREPOST to perform numerical transient analysis. LS-DYNA, is a general-purpose finite element code for analyzing the large deformation dynamic response of structures including structures coupled to fluids and is a commercial version of the public domain U.S. Department of Energy code DYNA3D (Whirley, 1993). The main solution methodology is based on explicit time integration and the explicit formulation is ideally suited for analyzing the dynamic response of structures subjected to impact loading. It has a robust suite of constitutive material models and contact surface algorithms. Spatial discretization is achieved by the use of elements such as 4-node tetrahedron elements, 8-node solid elements, 2-node beam elements, truss elements, membrane elements, discrete elements, and/or rigid bodies. Many material models (nearly 300 constitutive models and 10 equation of states) are available to represent a wide range of material behavior, including elasticity, plasticity, visco-elasticity, visco-plasticity, composites, thermal effects, and rate dependence. The FEA incorporated strain rate effects, non-linear geometry and material plasticity.

Results are presented below in Figure 56 through Figure 61. Midspan displacement of the roller shutter door panel was approximately 1830 mm at approximately 160 ms. Additionally, the axial force developed in the cable had a peak magnitude of approximately 8.7 kN at approximately 50 ms. Response of the door panel was similar in form to the pretest load analysis. The door panel velocity at the midspan was lower for the test load than for the design load. This is to be expected since the test impulse was on the order of 55% less due to leakage of the blast load.

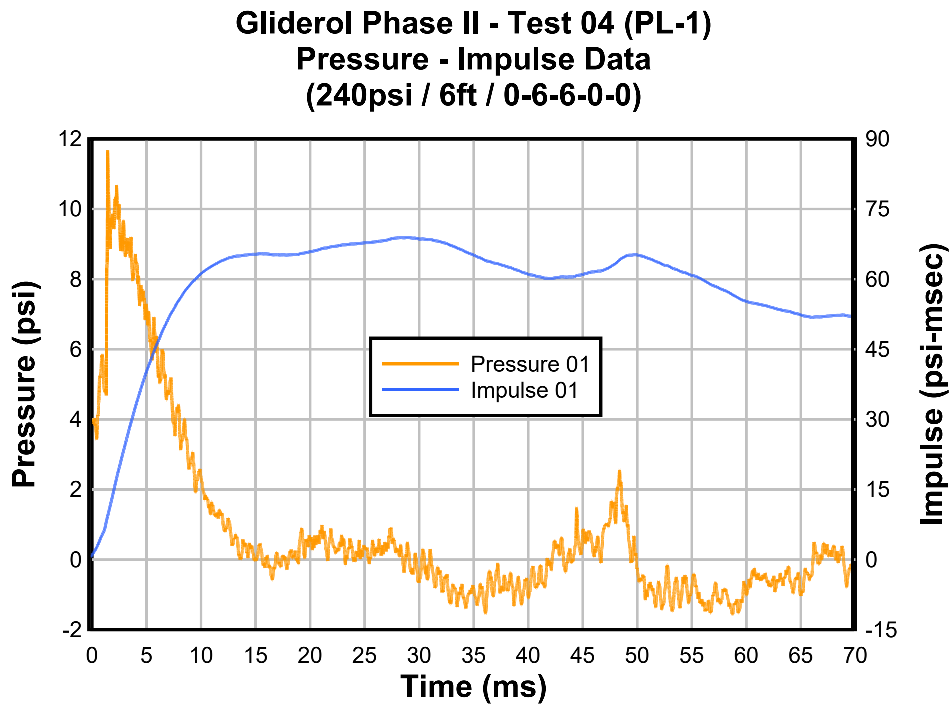

Figure 56 Test 04 Applied Blast Load (Includes Leakage)

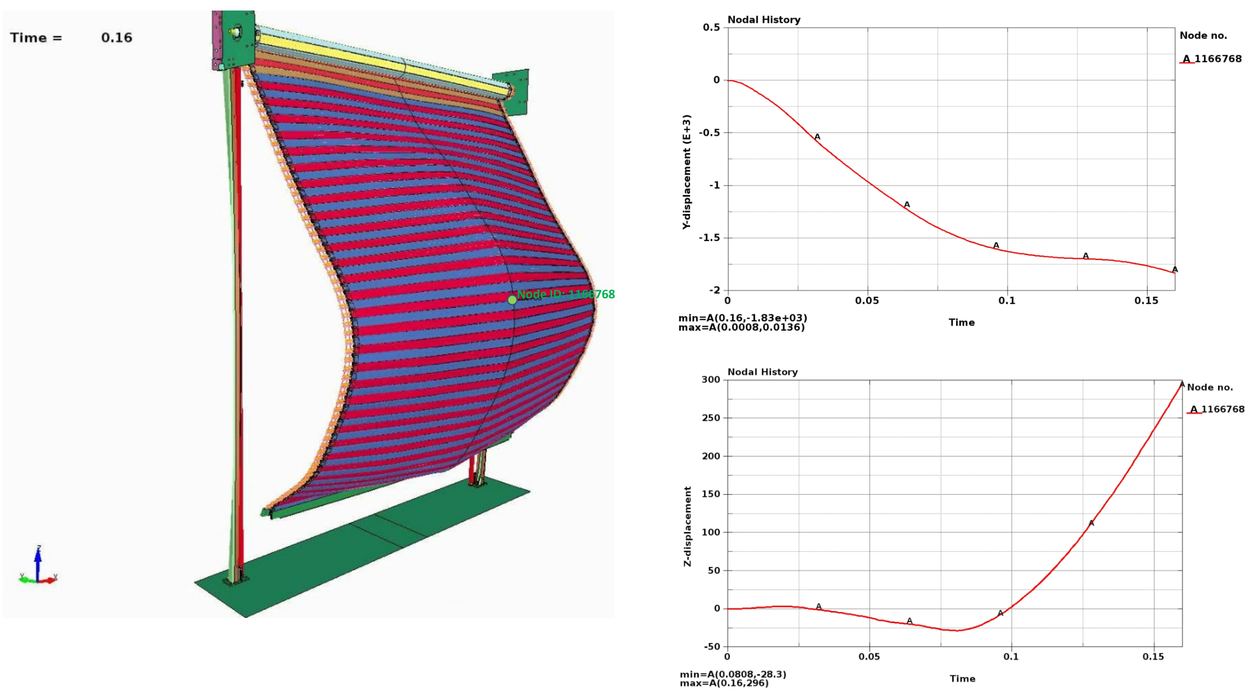

Figure 57 Test 04 Panel Midspan Displacement Time History (mm vs sec)

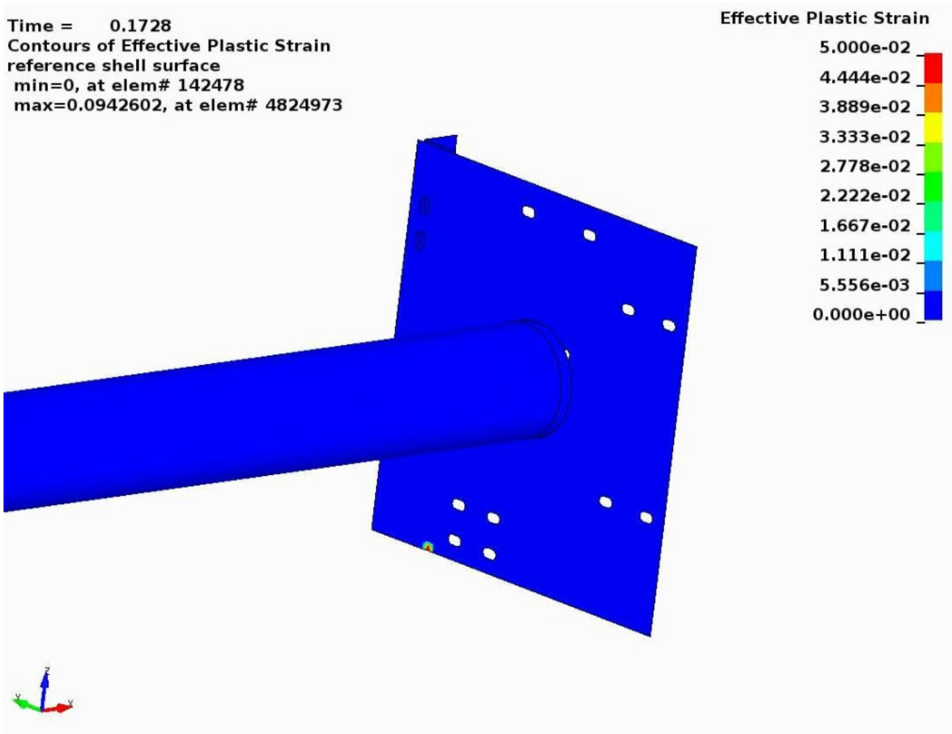

Figure 58 Test 04 Drum Maximum Effective Plastic Strain

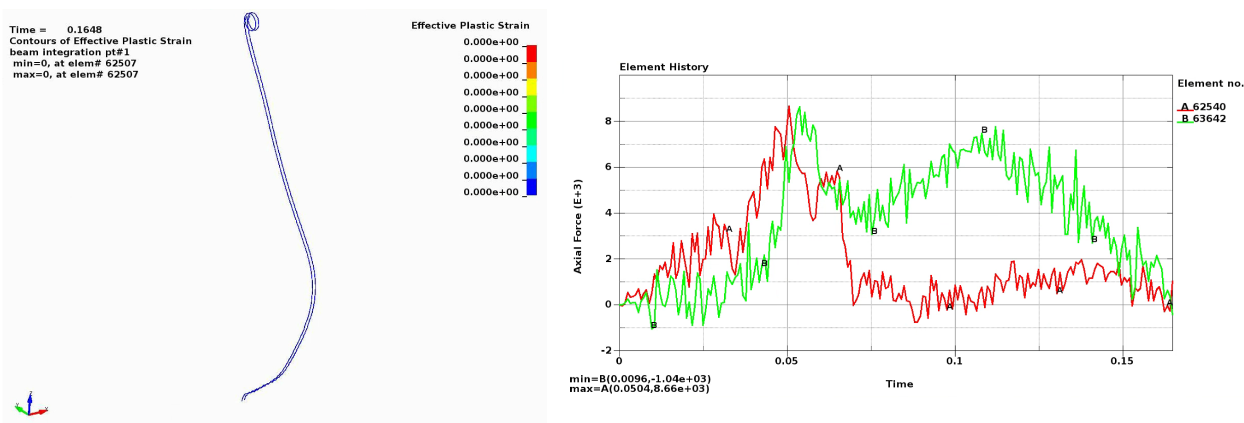

Figure 59 Test 04 Maximum Effective Plastic Strain and Axial Force (N) in Cable Ends

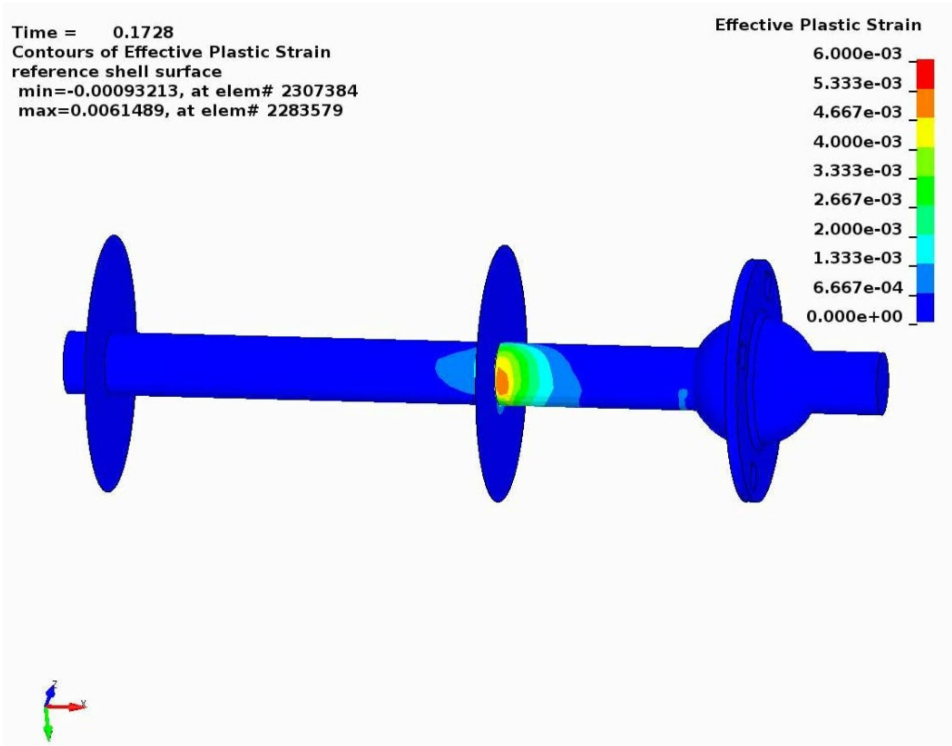

Figure 60 Test 04 Cumulative Plastic Strain in Drum Shaft

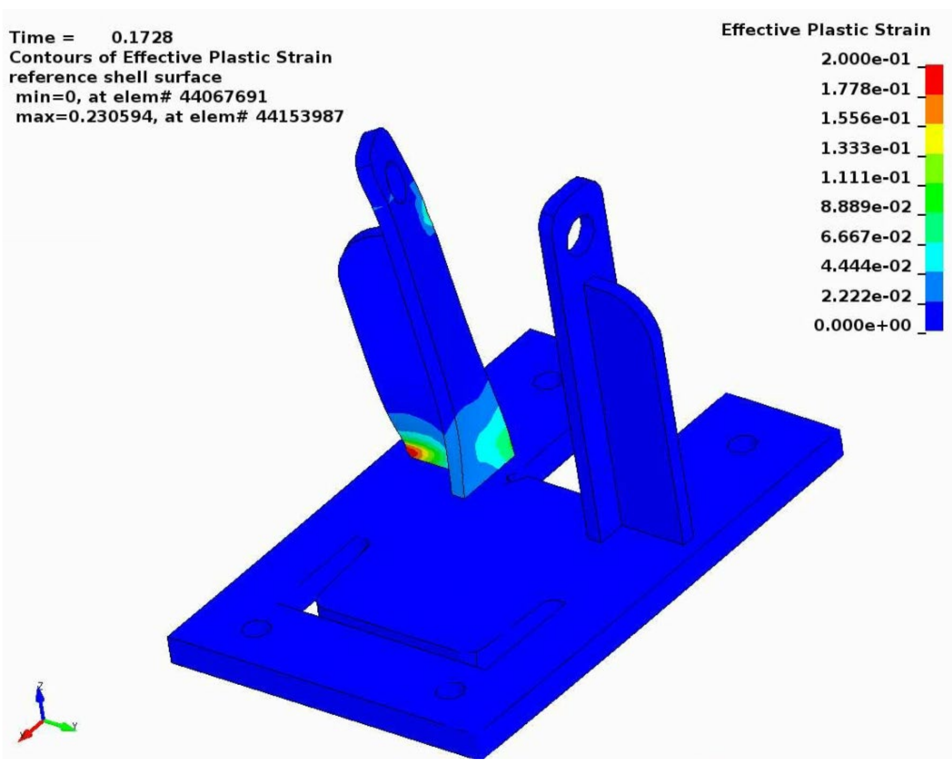

Figure 61 Test 04 Base Plate Cumulative Plastic Strain

4.2 PL 2 Simulation for Test 01 Measured Load

A simulation of the PL 2 configuration was prepared for the loads measured in Test 01. Changes to the design model were made for the post-test load analysis. These changes included addition of welds for the vertical capture channels which restrain the cable eyelets and addition of stiffeners for the restraint lugs at the base plate. Additionally, friction was included to reduce unspooling of the drum. Results are presented below in Figure 63 through Figure 68. Midspan displacement of the roller shutter door panel was approximately 511 mm at approximately 134 ms. Additionally, the axial force developed in the cable had a peak magnitude of approximately 9.4 kN at approximately 177 ms. Response of the door panel was similar in form to the design load analysis. The door panel velocity at the midspan was lower for the test load than for the design load. The test impulse was approximately 58% less due to leakage of the blast load.

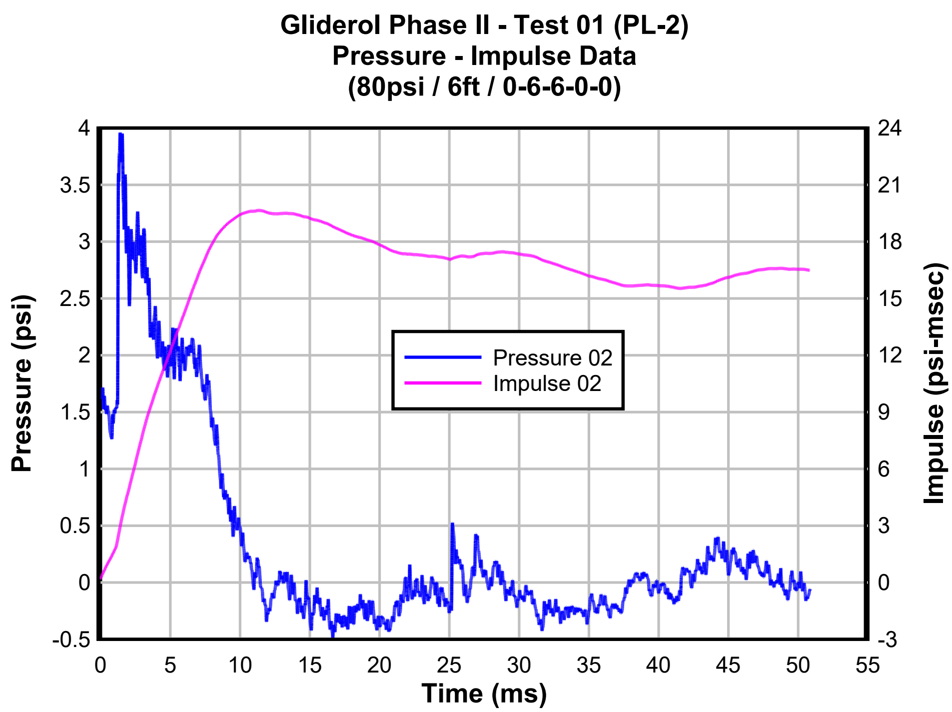

Figure 62. Test 01 Applied Blast Load (Includes Leakage)

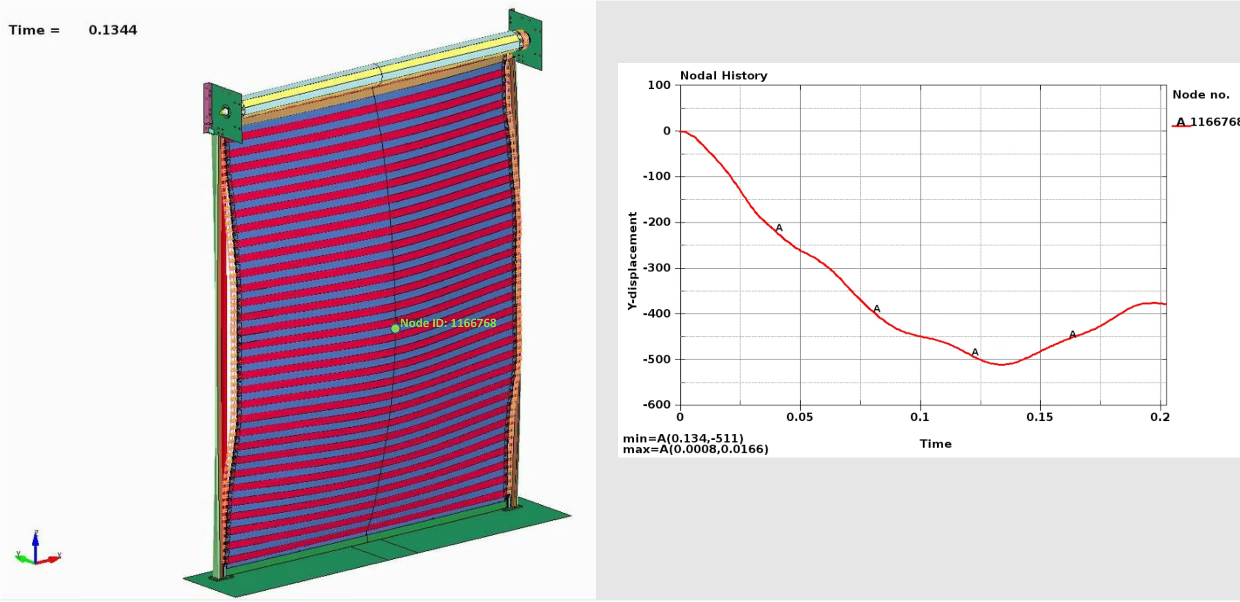

Figure 63. Test 01 Panel Midspan Displacement Time History (mm vs sec)

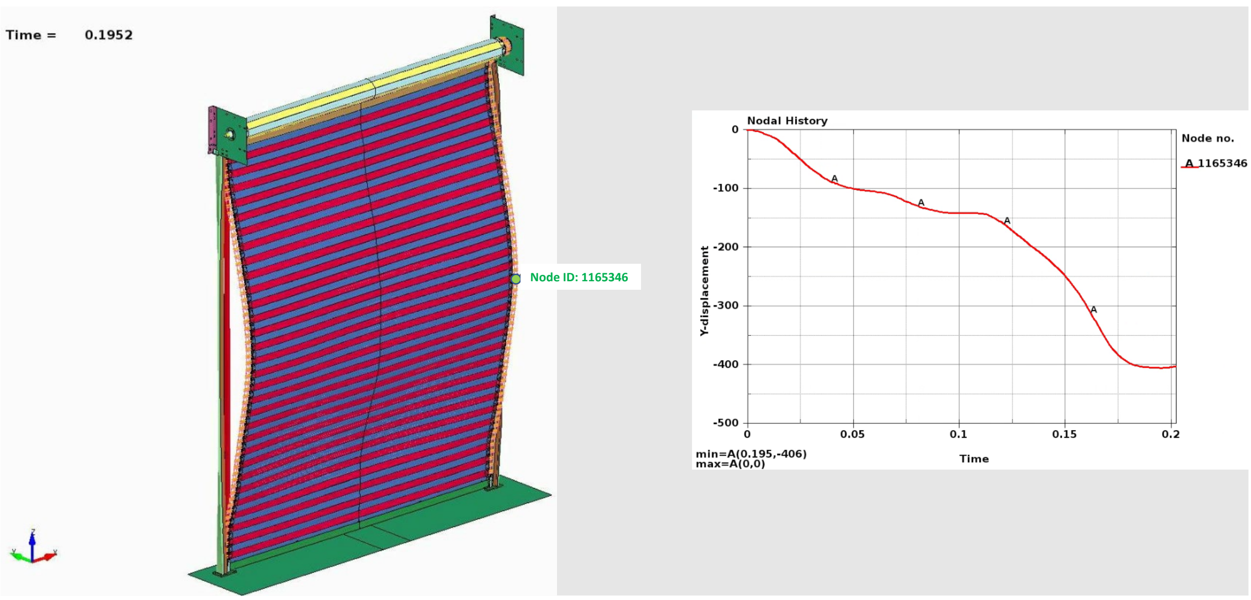

Figure 64. Test 01 Cable Midspan Displacement Time History (mm vs sec)

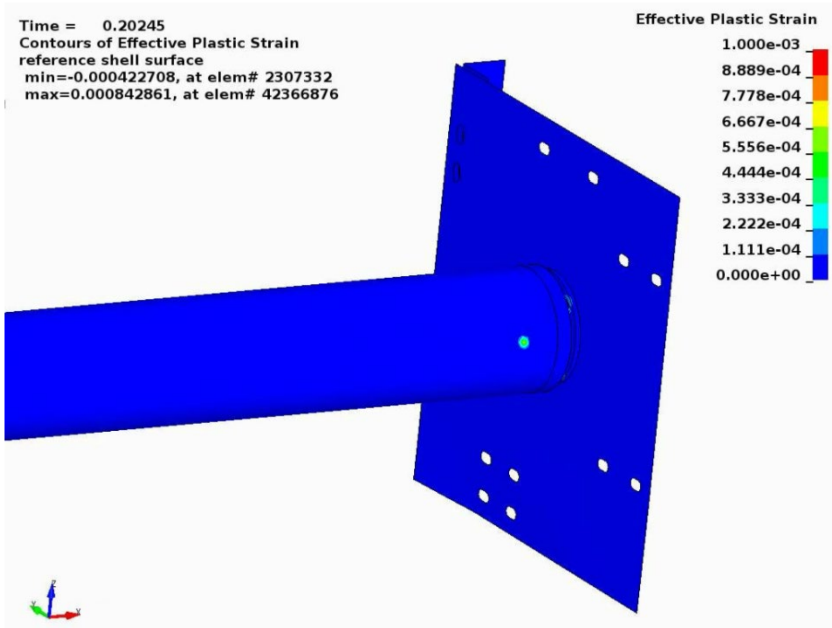

Figure 65. Test 01 Drum Maximum Effective Plastic Strain

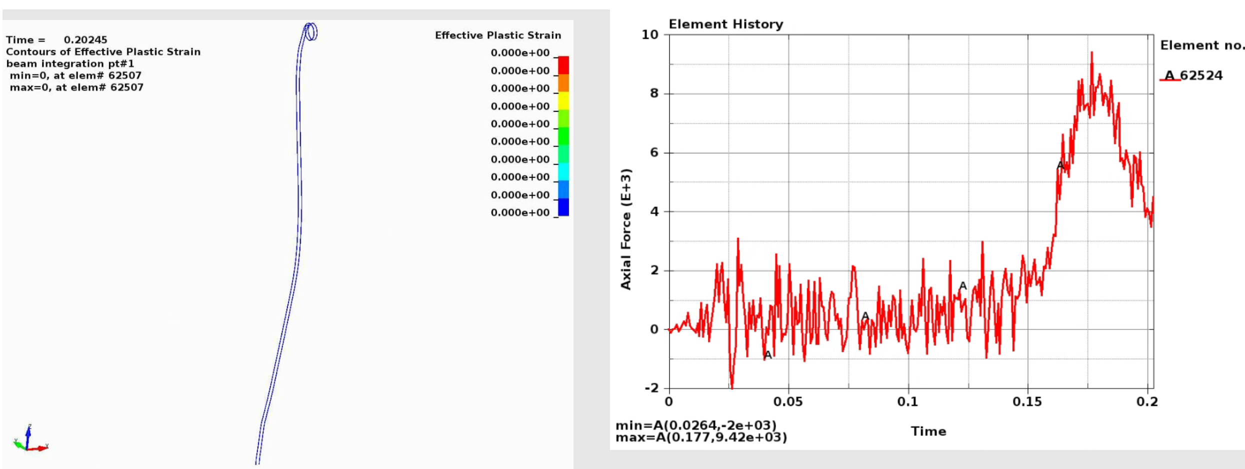

Figure 66. Test 01 Maximum Effective Plastic Strain and Axial Force (N) in Cable End

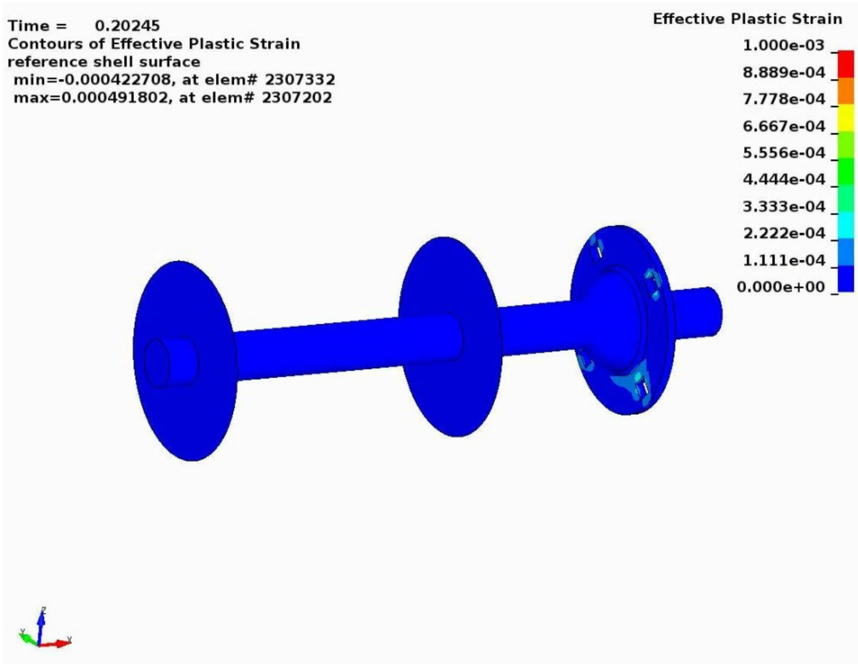

Figure 67. Test 01 Cumulative Plastic Strain in Drum Shaft

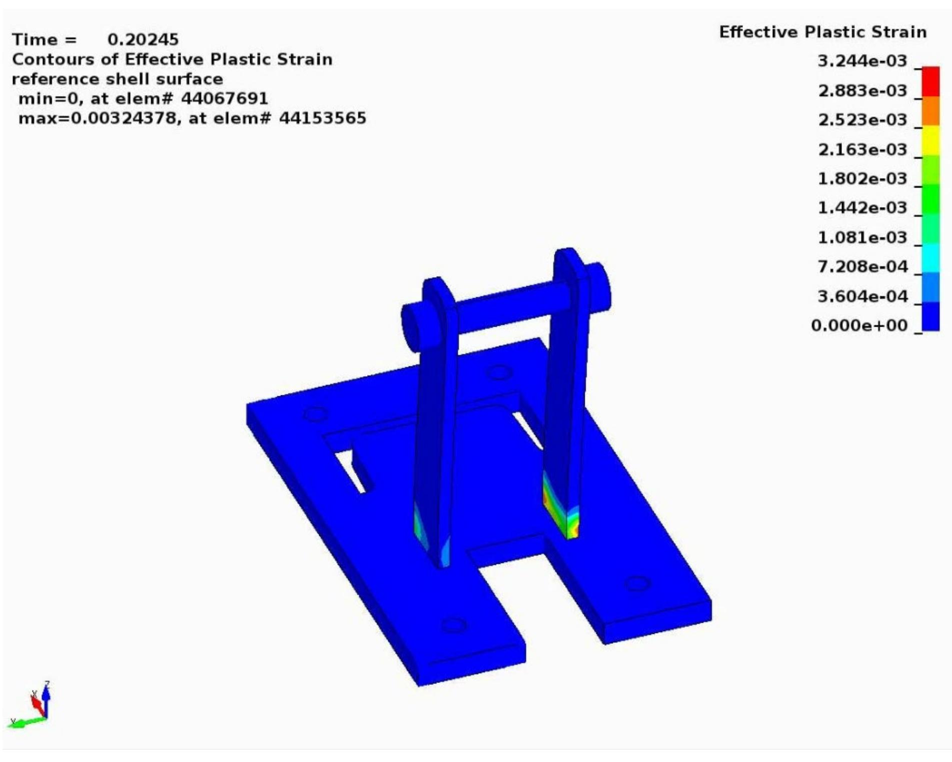

Figure 68. Test 01 Base Plate Cumulative Plastic Strain

5 Comparison of Physical Test with FEA Test Load Cases

A comparison of the measured door response in the test is made to the response in the FEA simulation of the loads measured in the test.

5.1 PL 1

Comparison of Test 4 response to the FEA model for measured test loads is provided in Figure 69 through Figure 72. The overall response time history of the door is very similar for test vs FEA as shown in Figure 71. The door panel horizontal displacement in the FEA simulation is within 8.3% difference of the test result at 144 ms. Variance in vertical door displacement is noted due to the cable shoe releasing from the pin restraint tab later in time in the FEA simulation. No failure of the door panel, cables, drum or mounting hardware is predicted in the FEA and is not observed in the test.

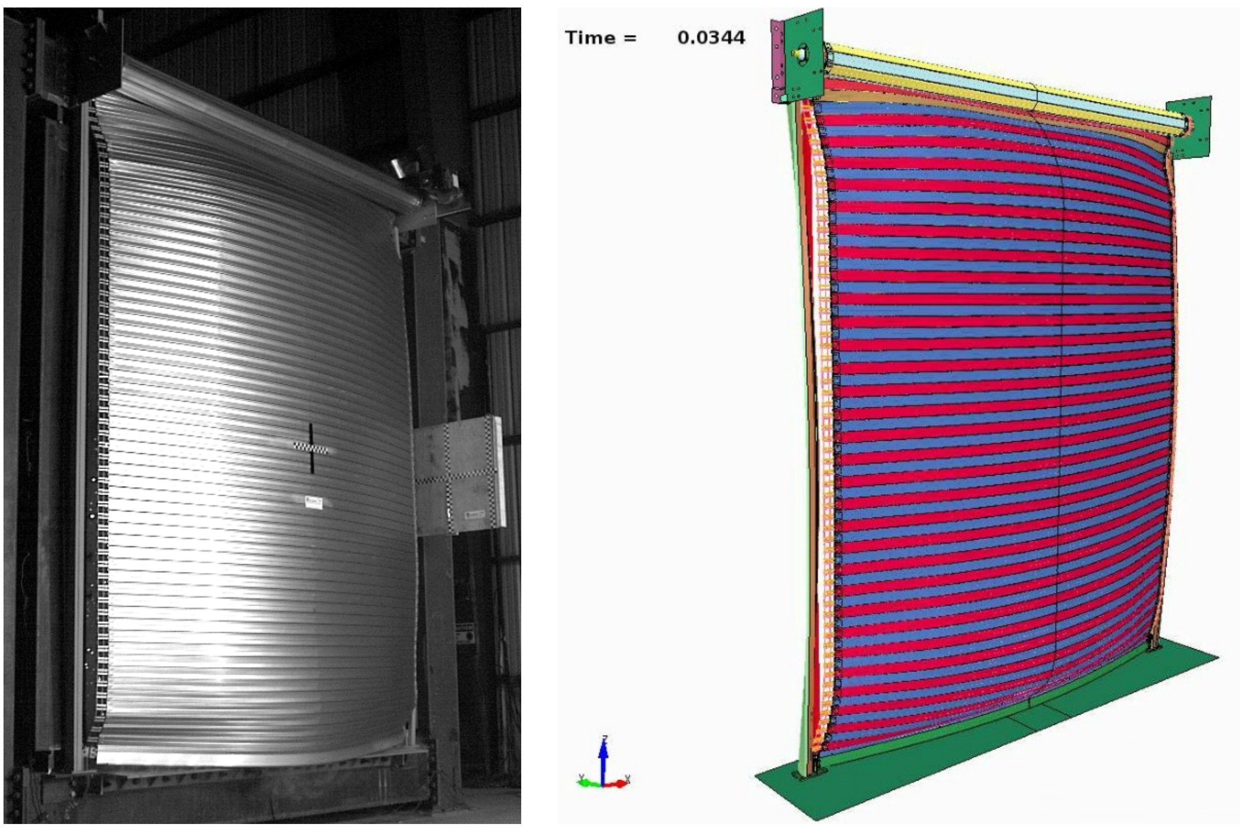

Figure 69 Test 04 Video vs FEA Displacement at 34 ms

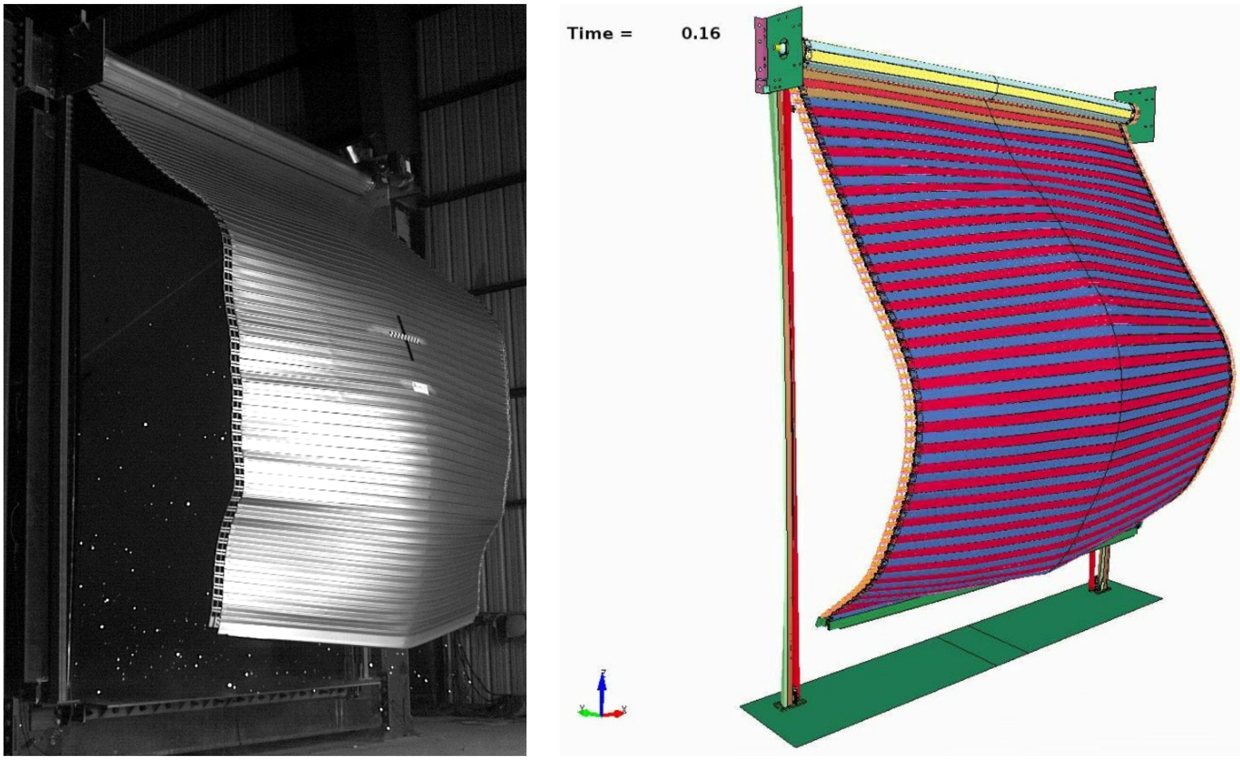

Figure 70 Test 04 Video vs FEA Displacement at 160 ms

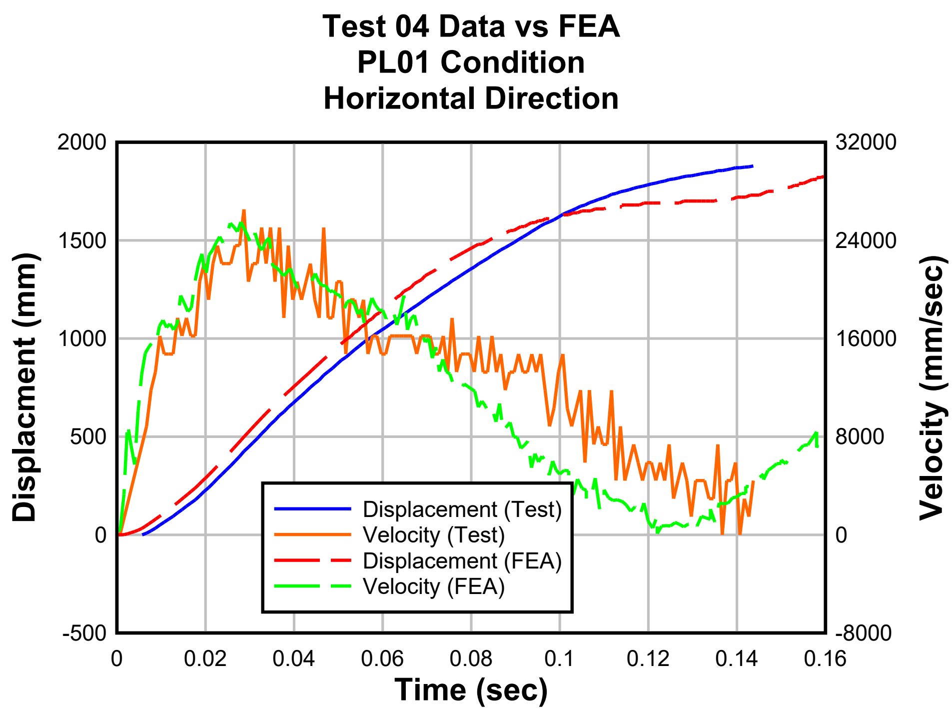

Figure 71 Test 04 Comparison of Highspeed Video to FEA Results at Midspan of Door – Horizontal Direction

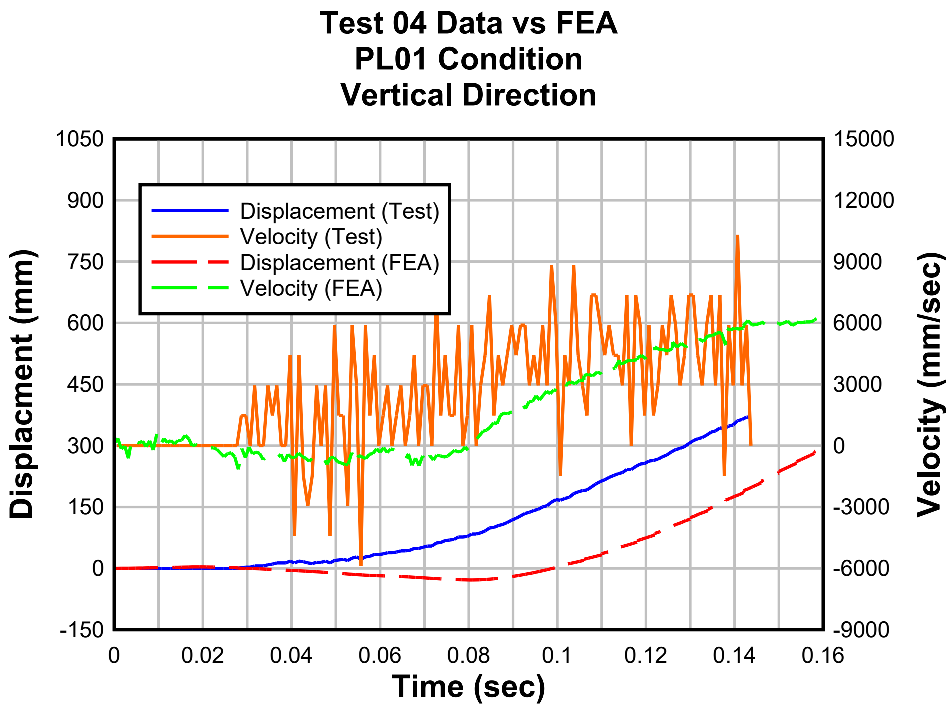

Figure 72 Test 04 Comparison of High-speed Video to FEA Results at Midspan of Door – Vertical Direction

5.2 PL 2

Comparison of Test 1 response to the FEA model for measured test loads is provided in Figure 73 through Figure 75. The overall response of the door is very nearly identical for test vs FEA as shown in Figure 75. The door panel displacement in the FEA simulation is within 4% difference of the test result. No failure of the door panel, cables, drum, restraining tabs or mounting hardware is predicted in the FEA and is not observed in the test.

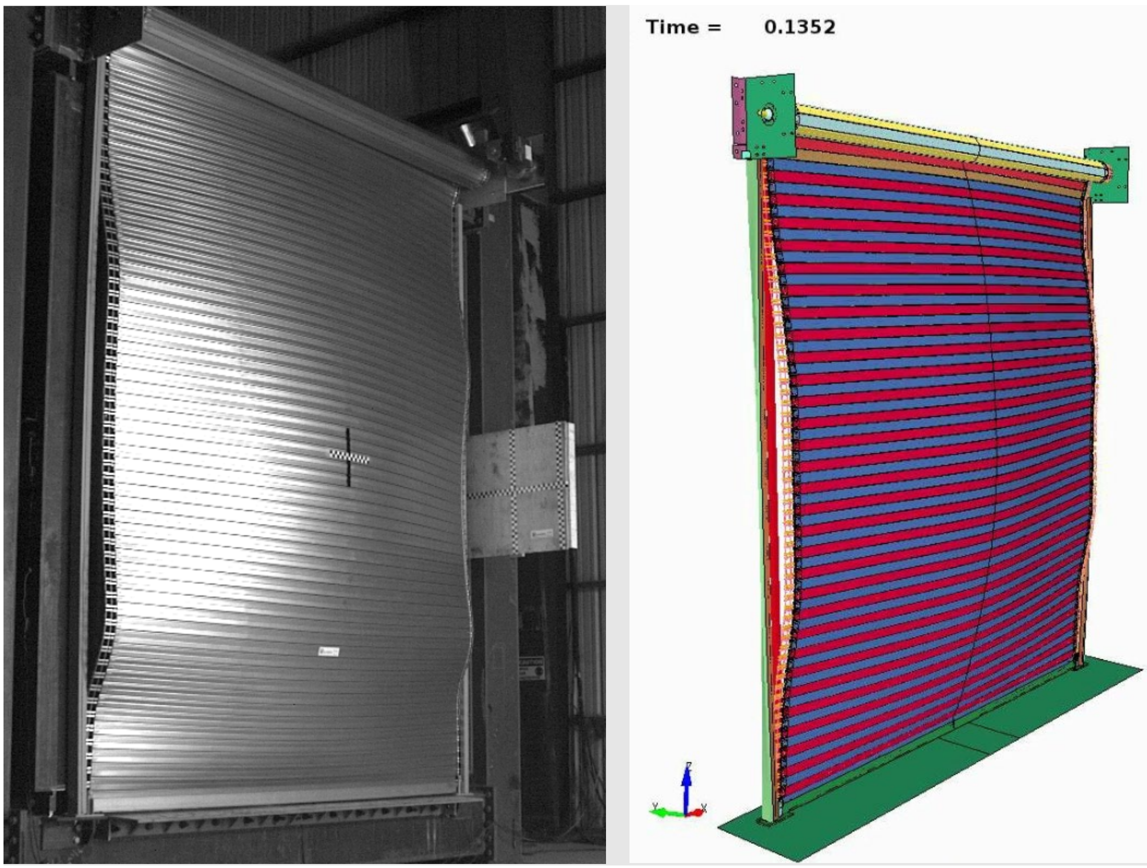

Figure 73. Test 01 Video vs FEA Displacement at 135 ms

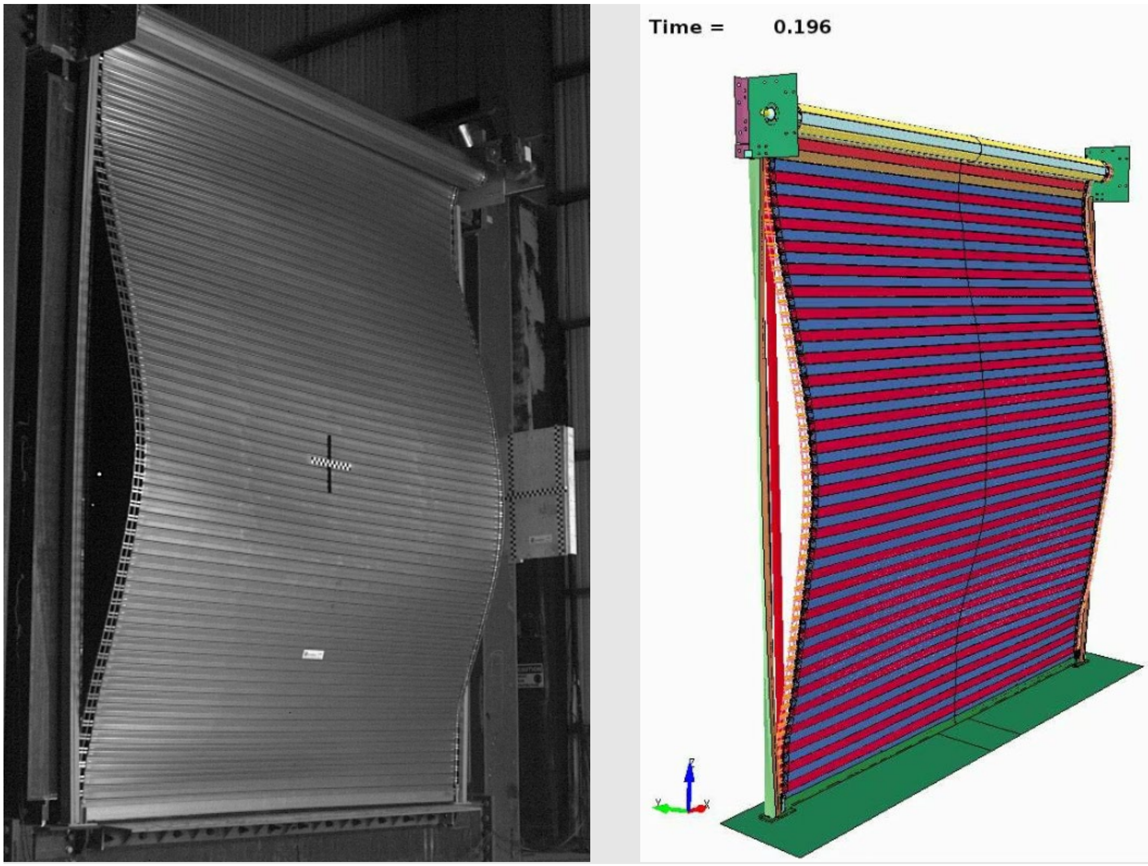

Figure 74. Test 01 Video vs FEA Displacement at 196 ms

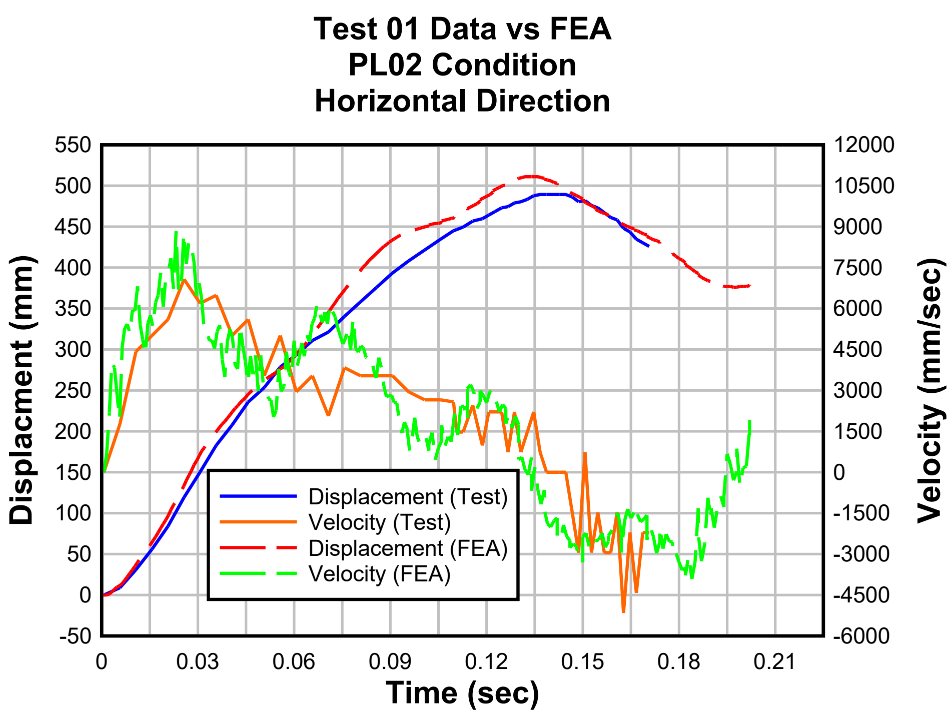

Figure 75 Test 01 Comparison of Highspeed Video to FEA Results at Midspan of Door – Horizontal Direction

6 Summary

The door test specimens performed well with both configurations meeting the target performance condition and load levels. Hardware used in the construction was robust as exhibited by the multiple tests conducted on each test article. The 8 mm rods were shown to have good ductility and failed in a manner which was expected from the analysis. The eyelet connectors proved to be sufficiently robust to completely develop the capacity of the cables. The panel construction was sufficient to prevent tear-out and other brittle modes of response. Minimal permanent damage was observed and no debris was produced.

The shock tube test results were in excellent agreement with the FEA analysis using the measured test loads for both PL 1 and PL 2 configurations (4-8%). These results indicate the FEA technique can reliably be used to develop future designs for alternate dimensions of blast loads.

The Blast Mitigating Shutter (PL 1) has been tested and shown to be capable of achieving limited permanent damage in response to a blast load with a peak pressure 75 kPA and peak impulse 1050 kPa-ms.

The Blast Resistant Shutter (PL 2) has been tested and shown to be capable of achieving limited permanent damage and be fully retained in response to a blast load with a peak pressure 40 kPA and peak impulse 500 kPa-ms.

7 References

Vision Research, Inc. PCC (Phantom Camera Control) Version 3.4.788.0. (n.d.).

Atlas of Stress-Strain Curves. (2002). Materials Park, OH: ASM International.

Johnson, G. R., & Cook, W. H. (n.d.). *A Constitutive Model and Data for Metals Subjected to Large Strains, High Strain Rates and High Temperatures.*

Kraemer, M. (2012). Testing and FEA Analysis of a Cable Supported Polycarbonate Shield System Against Glazing Hazards. *ASCE Structures Congress* (pp. 345-357). American Society of Civil Engineers.

Livermore Software Technology (LST), An Ansys Company. (2021). *LS-DYNA Keyword User's Manual.* Livermore, California: Livermore Software Technology.

Miscoe, A. a. (1993). *Wire Rope Research: Analysis of Bending Fatigue in a 2-inch IWRC Wire Rope, Report of Investigation 9466.* United State Department of Interior.

Seidt, J. D., Gilat, A., Klein, J. A., & Leach, J. R. (2007). High Strain Rate, High Temperature Constitutive and Failure Models for EOD Impact Scenarios. *Society of Experimental Mechanics (SEM) Annual Conference & Exposition on Experimental and Applied Mechanics.* Springfield, MA.

Steinberg, D. (1996). *Equation of State and Strength Properties of Selected Materials.* Livermore, CA: Lawrence Livermore National Laboratory.

Tabiei, A. (2015). *Fracture, Damage, and Failure in LS-DYNA.* Livermore, CA: Livermore Software Technology Corporation.

Whirley, R. a. (1993). *DYNA3D: A Nonlinear Explicit, Three-Dimensional Finite Element Code for Solid and Structural Mechanics, User Manual, Report USRL-MA-107254.* University of California, Lawrence Livermore Naitonal Laboratory.

Wire Rope Technical Board (WRTB). (2005). *Wire Rope Users Manual, 4th Edition.* Alexandria, Virginia.